

Mass Spectrometry Methods for Studying Structure and Dynamics of Biological Macromolecules

Lars Konermann,* Siavash Vahidi, and Modupeola A. Sowole

Department of Chemistry, The University of Western Ontario, London, Ontario, N6A 5B7 Canada

CONTENTS

Hydrogen/Deuterium Exchange	214
Fundamentals	214
Proteolytic Digestion-LC/MS	215
Characterization of Binding Interactions	216
HDX/MS of Intrinsically Disordered Proteins	216
Membrane Protein HDX/MS	217
Pulsed HDX/MS	217
Cytotoxic Protein Aggregates Studied by HDX/MS	218
Application of HDX/MS to Protein Therapeutics	218
Single Amide Resolution	218
HDX/MS with Electron-Based Fragmentation	218
Covalent Labeling	220
General Considerations	220
Hydroxyl Radical Labeling	220
Covalent Cross-Linking	222
ESI Charge State Distributions	222
ESI Mechanism for Folded Proteins	222
CID of Multiprotein Complexes	223
ESI Mechanism for Unfolded Proteins	223
“Supercharging” and Related Phenomena	224
Native Mass Spectrometry and Ion Mobility Spectrometry	224
Preservation of Native-Like Structures in the Gas Phase	224
Ion Mobility Spectrometry and Other Techniques for Probing Gas Phase Structures	224
Protein–Protein Complexes	225
Other Types of Noncovalent Assemblies	225
Concluding Remarks	227
Author Information	227
Corresponding Author	227
Notes	227
Biographies	227
Acknowledgments	227
References	227

All processes that occur within living organisms are intimately linked to biological macromolecules such as proteins, nucleic acids, or polysaccharides. Phospholipid membranes compartmentalize the interior of the cell and separate “inside” from “outside”. Elucidating the structures of all these biomolecular entities is an essential prerequisite for deciphering their role in health and disease. A comprehensive understanding of biological function also requires knowledge of conformational dynamics¹ and molecular interactions.^{2,3} X-ray crystallography,⁴ cryo-electron microscopy (EM),⁵ and nuclear magnetic resonance (NMR) spectroscopy⁶ are some of the key

methods that are routinely being applied for structural studies. In addition, a rapidly increasing number of research initiatives rely on the use of mass spectrometry (MS).⁷ The area of biological MS represents the focus of the current review. We will exclude the field of classical MS-based proteomics which mainly revolves around the identification and quantitation of proteins and their interaction partners.⁸ Instead, this review discusses the application of MS-based structural biology tools.⁹ Specifically, we will highlight methods that report on biomolecular conformations, dynamics, and binding mechanisms. In the following we will refer to these endeavors as *structural MS*. While attempting to provide a comprehensive overview, emphasis is placed on work conducted during the past 2 years. The overwhelming majority of structural MS studies have focused on proteins, and this is reflected in the choice of material that is being presented. Where appropriate, we will also mention results obtained for other types of biomacromolecules.^{10,11}

While nucleic acids are the blueprint of life, proteins represent the actual nanomachines that perform physiological tasks such as metabolic catalysis, energy conversion, host defense, and signaling. Within the area of protein structural biology, one can distinguish different themes. Newly synthesized protein chains have to fold into their biologically active (native) structures, a process that to this day remains a highly active research area.^{12,13} Intracellular folding may involve molecular chaperones that assist proteins in their conformational search toward the native state.¹⁴ Misfolding can result in the formation of cytotoxic aggregates, giving rise to a range of neurodegenerative diseases.^{15–17} Many native proteins are water-soluble, with a tightly folded globular structure that is characterized by a hydrophobic core and a hydrophilic exterior. Additionally there is large number of intrinsically disordered proteins (IDPs) that act as versatile binding partners in signaling cascades.^{18–21} Protein therapeutics comprise modified monoclonal antibodies and other soluble species.^{22–24} For many years the pharmaceutical market has been dominated by low molecular weight (MW) synthetic compounds, but in 2011 32% of all new drugs approved by the U.S. Food and Drug Administration were protein-based.²⁵ Integral membrane proteins (IMPs) are situated within lipid bilayers. Their largely hydrophobic exterior makes them prone to aggregation. From an experimental perspective IMPs are generally considered to be the most challenging class of proteins,²⁶ and only relatively

Special Issue: Fundamental and Applied Reviews in Analytical Chemistry 2014

Received: December 3, 2013

Published: December 4, 2013



few high resolution IMP structures have been reported. This is despite the fact that IMPs are among the most important drug targets.²⁷ It will be seen that structural MS can provide important insights into all of these areas.

Electrospray ionization (ESI)²⁸ and matrix-assisted laser desorption/ionization (MALDI)²⁹ both allow the production of intact gaseous ions from macromolecular analytes for MS. MALDI and related techniques are very useful for imaging and many other applications.^{30,31} However, for most structural investigations, ESI-MS eclipses MALDI-MS. The main advantage of ESI is the facile coupling with liquid chromatography (LC) which allows the separation of protein digests, thereby reducing the complexity of the data obtained. Also, many structural MS applications benefit from the fact that ESI (or its low-flow variant, nanoESI³²) provides a direct bridge between solution phase chemistry and gas phase detection. In addition, the relatively high charge states produced by ESI facilitate MS/MS experiments that involve collision-induced dissociation (CID),³³ electron capture dissociation (ECD),³⁴ or electron transfer dissociation (ETD).^{35,36} MS/MS is essential for peptide identification and for pinpointing the position of modification sites. The workflow in these studies usually follows a “bottom-up” approach, where the macromolecular analyte is first cleaved enzymatically in solution, followed by MS/MS interrogation of the resulting segments. Trypsin is by far the most widely used protease for these studies due to its extremely high cleavage specificity on the C-terminal side of Arg and Lys.³⁷ In contrast, most other proteases are more promiscuous in their choice of cleavage sites, thus increasing the likelihood of false peptide identifications in complex samples. MS measurements can also be conducted in a “top-down” fashion that involves the fragmentation of intact macromolecular analytes in the vacuum of the mass spectrometer without prior enzymatic cleavage.^{38,39} CID, ETD, and ECD can all be employed for top-down studies. In addition, ultraviolet photodissociation (UVPD) is an interesting emerging tool.⁴⁰ “Middle-down” MS represents an intermediate regime where gas phase fragmentation is applied to large digestion products.⁴¹

From a novice’s point of view it may seem counterintuitive that MS can be used for conformational studies on proteins and other macromolecular analytes. After all, structural transitions *per se* are not associated with a change in *m/z*, as they only involve the rotation of σ bonds (e.g., polypeptide Ψ/Φ backbone angles). Nonetheless, there are numerous exquisitely sensitive strategies for interrogating structural changes via mass shift readouts.^{7,42} Solution-phase labeling alters the analyte mass in a conformation-dependent fashion. Macromolecular structures that are disordered and/or unfolded tend to undergo more extensive labeling than tightly folded conformers. This simple idea forms the basis of hydrogen/deuterium exchange (HDX) and covalent labeling experiments. Similarly, unfolded protein conformers tend to bind more protons during ESI, such that charge state distributions can be used to probe structural changes in solution. Covalent cross-linking reports on inter- and intramolecular distances. Ion mobility spectrometry (IMS) provides information on analyte shapes via collision cross section (CCS) measurements in the gas phase. Information on receptor–ligand and quaternary interactions comes from “native” ESI-MS measurements that allow the detection of intact supramolecular complexes in the gas phase. All of these approaches will be discussed in more detail below.

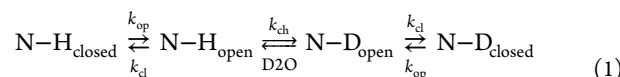
Before highlighting individual techniques in more detail it is worthwhile to briefly consider a basic point. Structural MS involves the detection of ions *in the gas phase*, whereas most studies employing this approach aim to characterize the behavior of analytes *in solution*. This issue is of little concern for studies that simply require a mass readout following solution phase covalent modifications, cross-linking, or HDX. Yet, other approaches such as native ESI-MS or IMS rely (to a certain extent) on the assumption that solution phase structure is preserved in the gas phase. The validity of this supposition is a hotly debated topic^{43,44} that we will return to toward the end of our review.

■ HYDROGEN/DEUTERIUM EXCHANGE

Fundamentals. Amide backbone HDX has become the method of choice for many laboratories interested in studying the structure and dynamics of proteins (for recent reviews see refs 45–50). The secondary structure of proteins is stabilized by backbone N–H...O=C hydrogen bonds. Exposure to a D₂O-containing solvent environment induces the replacement of backbone hydrogen (more accurately, “protium”, i.e. ¹H) atoms with deuterium (²H). The ~1 Da mass difference between hydrogen and deuterium allows the tracking of HDX events by MS. Measurements are usually conducted under exchange-in conditions where an initially unlabeled protein is incubated in D₂O. Alternatively, exchange-out experiments can be conducted that involve the exposure of a fully deuterated protein to H₂O. Both types of experiments yield basically the same information.

HDX also takes place at O–H, N–H, and S–H side chain sites, but this deuterium is lost due to back exchange during the digestion and LC steps and thus does not contribute to the measured mass shifts in typical proteolytic digestion HDX/MS experiments.⁵¹ The slowly exchanging imidazole C₂–H of His represents a possible exception. The unusual deuteration behavior of His can be exploited for thermodynamic stability measurements.⁵² Unexpected deuterium retention has been reported for glycan sites.⁵³ The latter observation points to future opportunities for HDX/MS measurements on the structure and dynamics of polysaccharides, but thus far this potential resource remains untapped.

The mechanism of backbone HDX for native proteins under continuous-labeling conditions is usually expressed via eq 1, building on ideas that were first expressed by Linderstrom-Lang et al. more than 50 years ago.⁵⁴ This mechanism assumes that exchangeable backbone sites fluctuate between “closed” (exchange incompetent) and “open” (exchange competent) sites. The interconversion kinetics are governed by the corresponding rate constants k_{op} and k_{cl} . Once the open state is reached, deuteration proceeds with the rate constant k_{ch} .



Most HDX studies assume that the biophysical properties of proteins are virtually indistinguishable before and after deuteration. Overall this notion seems to be valid, although there continue to be reports of subtle alterations in the structure, dynamics, and catalytic efficiency of deuterated proteins.⁵⁵ Studies on small model systems suggest that D-bonds are somewhat stronger than H-bonds, but depending on the molecular context this trend can be reversed.⁵⁶ Certainly, HDX represents the most benign of any protein labeling

techniques, especially when compared to the covalent tagging approaches that will be discussed in the subsequent chapter.

In the commonly encountered EX2 regime (characterized by $k_{\text{cl}} \gg k_{\text{ch}}$) the first-order HDX rate constant is given by

$$k_{\text{HDX}} = \frac{k_{\text{op}}}{k_{\text{cl}}} k_{\text{ch}} \quad (2)$$

EX2 kinetics manifest themselves via peak envelopes that gradually shift to higher m/z as the D_2O exposure time increases. In contrast, EX1 kinetics ($k_{\text{cl}} \ll k_{\text{ch}}$) usually lead to bimodal mass distributions.^{45–49} Practitioners have to be careful in identifying this EX1 regime, as sometimes sample carryover during LC can give rise to false EX1 signatures.⁵⁷

The mechanism expressed in eq 1 emphasizes the role of HDX/MS as a tool for probing thermally activated structural dynamics. Yet, the exact nature of the opening/closing events invoked here remains under discussion. NMR data suggest that for exchange to happen, the hydrogen bond of interest has to be disrupted for a short period of time and the N–H has to come in contact with the D_2O solvent.⁵⁸ This interpretation contrasts the view frequently found in the MS literature, where solvent accessibility in the native state is cited as a primary determinant of HDX kinetics. MD simulations are a potentially useful tool to better understand the exact nature of opening/closing events and their relationship to HDX rates. Work in this direction is off to a promising start,^{59–61} but the problem is far from being solved. DXCOREX is a computer algorithm that predicts HDX kinetics on the basis of protein structural models. It has been suggested that this tool can be used for assessing the validity of computer-derived structure predictions, effectively turning HDX/MS into a tool for determining the three-dimensional conformation of proteins.⁶²

While the opening/closing transitions in eq 1 occur on time scales down to the microsecond range, HDX half-lives of natively folded proteins range from minutes to days, as governed by the magnitude of $k_{\text{op}}/k_{\text{cl}}$ in eq 2.⁵⁸ It is possible to modulate the HDX kinetics, taking advantage of the pD dependence of k_{ch} which is given by⁶³

$$k_{\text{ch}} = k_{\text{A}}[\text{D}^+] + k_{\text{B}}[\text{OD}^-] + k_{\text{W}} \quad (3)$$

Equation 3 reflects the fact that HDX can proceed with catalysis by acid, base, and water. In near-neutral solution, base catalysis is the dominant mechanism. According to eqs 2 and 3 it is possible to alter the k_{HDX} values of a natively folded protein and move the kinetics into a range that best suits the experimental time window, simply by changing pD.^{64,65} Care has to be taken, however, that these pD changes do not affect the structure and dynamics of the protein.

Proteolytic Digestion-LC/MS. Most HDX/MS investigations follow a bottom-up approach, building on ideas that were developed in the early 1990s.^{66,67} Two of the pioneers in this area, Virgil Woods⁶⁸ and Max Deinzer⁶⁹ passed away unexpectedly in 2012 and 2013, respectively. A range of mass analyzers can be used for these experiments, including Fourier-transform-based systems (ion cyclotron resonance and Orbitrap instruments) as well as quadrupole-time-of-flight (Q-TOF) mass spectrometers.^{70,71} For traditional continuous-labeling experiments, the protein of interest is incubated in D_2O , typically at neutral pH and in the presence of buffers and salts. Aliquots are removed at selected labeling times, ranging from a few seconds to several days. Labeling is quenched by cooling to $\sim 0^\circ\text{C}$. In addition, the pH is lowered to ~ 2.5 which drastically

reduces the magnitude of k_{ch} (eq 3). The solution is then passed through a column containing surface immobilized pepsin or another acid-active endoprotease, cleaving the protein into numerous peptides. The application of high pressures during proteolysis can enhance the digestion efficiency.^{72,73} The resulting peptides are retained on a short trapping column and subsequently transferred to an analytical column for reverse-phase LC. Retention time alignment tools help improve the reproducibility of this peptide separation step.⁷⁴ Sample carryover due to undesired analyte retention, particularly in the digestion column, can be minimized by appropriate washing.^{57,75} Because of the nonspecific nature of pepsin and other acid proteases, the identity of all digestion products has to be verified by MS/MS. Pepsin activity is severely affected by the presence of disulfide bonds, requiring the application of protocols that allow digestion and disulfide reduction to be carried out simultaneously.^{76,77} The availability of commercial systems that perform LC/MS-based HDX/MS measurements in an automated fashion has helped to make this technique accessible to a large user base.⁷⁸ Nonetheless, state-of-the-art measurements can also be conducted using custom-built devices.⁷⁹ The general layout of a typical digestion/desalting/separation fluidics unit for HDX/MS is depicted in Figure 1. A number of software packages have become available that can aid with data analysis, addressing one of the key bottlenecks of the HDX/MS workflow.^{47,70,80–84}

The implementation of lab-on-a-chip HDX systems is an interesting recent development,^{85,86} although those miniaturized systems often lack certain components of the workflow described above. MALDI-MS remains a viable option for HDX-MS measurements as well, despite the absence of an LC-based peptide separation step.⁸⁷

A key challenge in HDX/MS is the occurrence of back exchange during digestion, peptide trapping, and separation. Back exchange tends to wash out the deuteration pattern imprinted on the protein during labeling.⁸⁸ Complete deuterium loss in *side chains* is actually beneficial, because it removes a large deuteration background. Unfortunately, back exchange also takes place for the structurally informative backbone amides, requiring the digestion and LC workflow to be conducted very rapidly (within tens of minutes or less) and at 0°C . The use of freezing point depressants for subzero degree fluidics has been demonstrated, resulting in significantly improved deuterium retention.^{85,89} Also, careful optimization of the mobile phase ionic strength can reduce the extent of back exchange.⁹⁰ The application of millisecond digestion protocols in this context would be highly beneficial.⁹¹

Porcine pepsin remains the most widely used protease for HDX/MS because of its relatively high efficiency under acidic quench conditions. Unlike trypsin (which is inactive at low pH), pepsin cleaves rather nonspecifically, requiring the identification of each hydrolysis product by MS/MS prior to the actual HDX experiments. Systematic exploration of peptic cleavage patterns has nonetheless revealed some trends that can aid at the peptide identification stage. For example, cleavage takes place preferentially after Phe and Leu but never after His, Lys, Arg, or Pro.^{92,93} There is an ongoing quest to identify alternative acidic proteases that provide cleavage patterns complementary to those of pepsin.⁹³ Nepenthesin is a promising candidate due to its very high activity and the capability to cleave after the “pepsin-forbidden” residues His, Lys, Arg, or Pro.⁹⁴

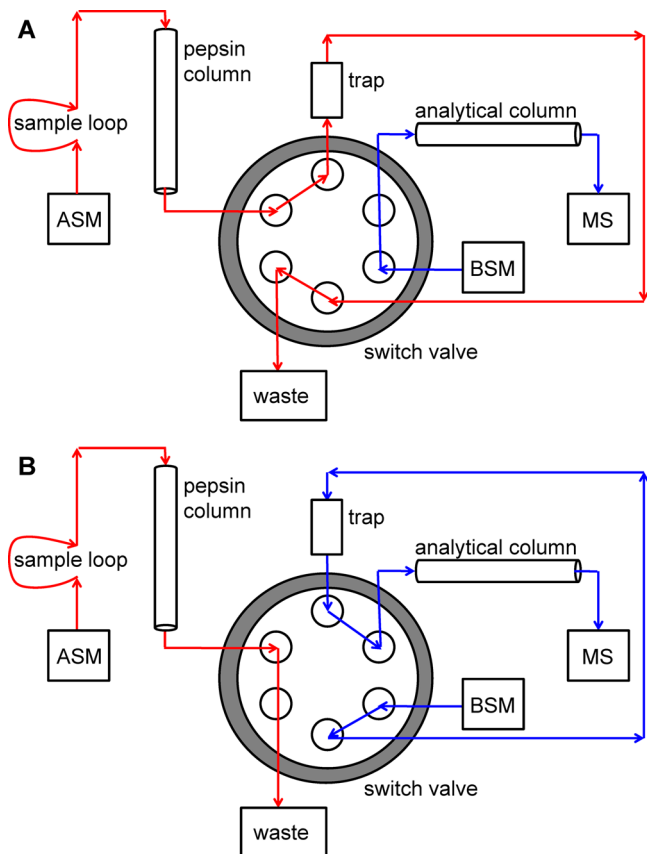


Figure 1. Layout of a typical fluidics unit for “bottom-up” proteolytic digestion HDX/MS experiments. (A) Isocratic flow (red) delivered by an auxiliary solvent module (ASM) moves the protein from the sample loop to a pepsin column for digestion. The resulting peptides are retained on a short trapping column. (B) Switching of the six-port valve allows the proteolysis products to be washed off the trapping column via flow from a binary solvent module (BSM) which delivers a water/acetonitrile gradient (blue). The peptides are separated on a reversed-phase analytical column that is coupled to the ESI source of a mass spectrometer (MS).

Characterization of Binding Interactions. HDX/MS provides a highly sensitive fingerprint of protein structure and dynamics. Probably the most informative approach, however,

lies in the application of HDX/MS for *comparative analyses* of a protein under different conditions. In this way it becomes possible to pinpoint protein region(s) that are most responsive to changes in certain variables. One application of this kind is the comparison of genetic variants.⁹⁵ An even more widely used type of experiment involves the characterization of protein–protein or protein–ligand interactions.^{49,96} In such studies the protein of interest is incubated by itself and in the presence of its binding partner. Butterfly or mirror plots are one way of comparing the HDX behavior of free and bound protein.⁹⁷ Recent examples of such investigations include studies on protein–DNA binding,^{98,99} interactions of antibodies with a membrane-bound HIV segment,¹⁰⁰ phospholipase inhibition,⁶¹ as well as lipid-induced protein conformational changes.¹⁰¹

Binding of a protein to a ligand usually stabilizes the protein structure, i.e., it causes a reduction in $k_{\text{op}}/k_{\text{cl}}$ that induces a decrease of k_{HDX} (slower exchange, eq 2).^{46,102,103} Some proteins exhibit ligand-induced stabilization only in some domains, whereas other regions become destabilized upon binding.^{104–107} It is tempting to use HDX/MS for mapping binding sites, implicitly postulating that the largest reduction in structural dynamics will occur where protein and ligand interact. Unfortunately, such a simplistic data interpretation can be misleading because protein binding interactions often involve allosteric effects, where major effects occur far away from the site of interaction.^{49,96} Careful consideration of this possibility is of particular importance for the interpretation of HDX/MS-based epitope mapping experiments.¹⁰⁸

The occurrence of allosteric effects and ligand-induced stabilization/destabilization has recently been demonstrated for the bacterial protease ClpP, a 14-subunit complex that undergoes activation by binding to Acyldepsipeptide 1 (ADEP1).¹⁰⁹ The 14 ligand binding sites are arranged in two concentric rings around the axial pores of the complex. In the presence of ADEP1 the binding regions exhibit increased HDX rates. A pronounced rigidification is seen in the equatorial segments of the complex, i.e., far removed from the binding sites (Figure 2). These HDX/MS data provide detailed insights into the mechanism of ADEP1-mediated activation.¹⁰⁵

HDX/MS of Intrinsically Disordered Proteins. IDPs are a class of proteins that defy the classical structure–function paradigm, according to which a well-defined structure is required for biological function. While the free state of these

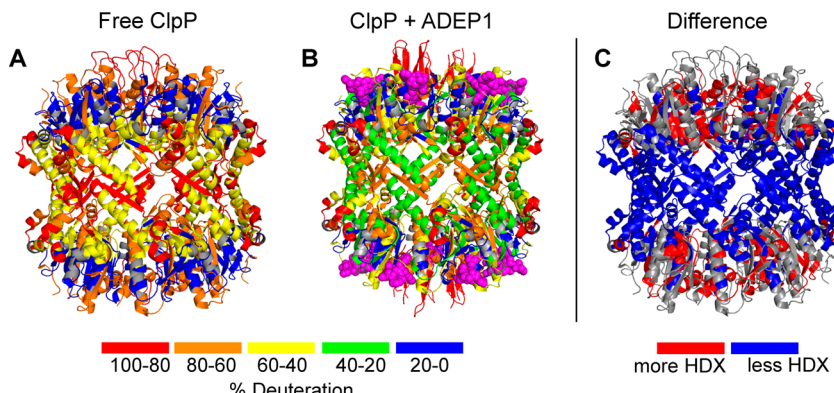


Figure 2. HDX behavior of the ClpP proteolytic complex in the absence (A) and presence (B) of the activator ADEP1. The two axial pores that provide substrate access to the central digestion chamber are pointing toward the top and bottom. In panel B bound ADEP1 ligands are depicted in pink. Colors in parts A and B represent the extent of HDX after 1 h of D₂O incubation. (C) HDX difference map. Red regions get destabilized, whereas blue regions become more rigid upon ADEP1 binding. Reprinted with permission from ref 105. Copyright 2013 Elsevier.

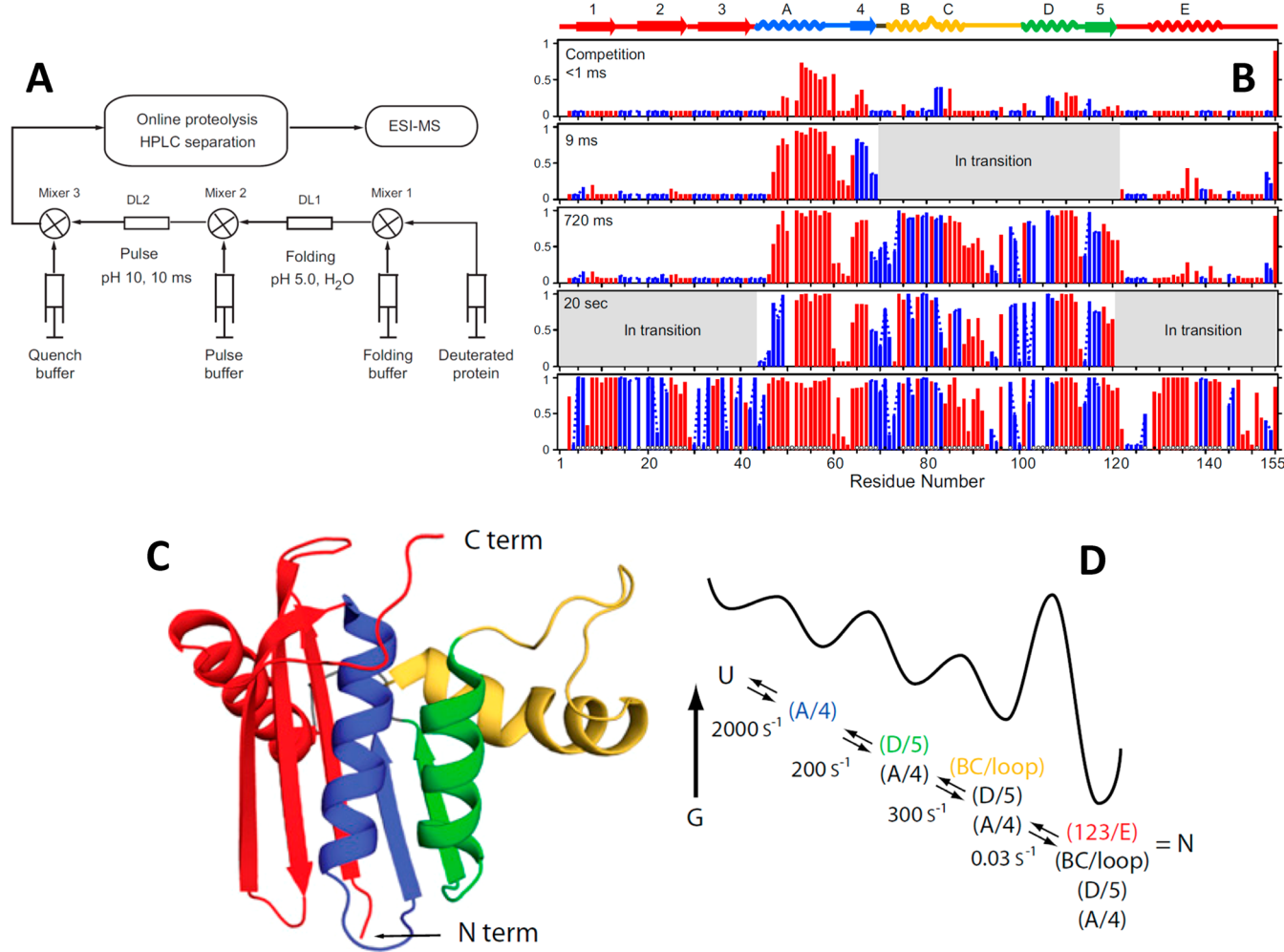


Figure 3. Exploring the folding mechanism of ribonuclease H1 by pulsed HDX/MS. (A) Experimental setup with three sequential mixers for initiation of folding, starting, and stopping of the labeling pulse. DL1 represents a variable delay (milliseconds to seconds), whereas DL2 is a constant 10 ms delay. This experiment was carried out under exchange-out conditions, i.e., ¹H labeling of an initially deuterated protein. (B) Deuteration patterns for folding time points of 1 ms, 9 ms, 720 ms, 20 s, and for the native protein. The y-axes display the deuterium retention of backbone amide sites. A value of unity represent complete protection, i.e., a folded segment. Regions for which single residue resolution was obtained are depicted in red, others are shown in blue. Regions marked “In transition” exhibit bimodal mass distributions that could not be analyzed. (C) Structure of the native protein. The four folding units “foldons” are highlighted in color. (D) Linear folding pathway and free energy profile with barriers and local minima. The blue unit folds first, followed by green, yellow, and red. The last step has the highest activation barrier and is therefore rate-determining. Reprinted with permission from ref 121. Copyright 2013 National Academy of Sciences of the United States of America.

proteins is highly disordered, many of them undergo folding after binding to interaction partners. Disorder in the free state does not always extend over the entire sequence but may be confined to certain regions.^{18–20} HDX/MS is increasingly being used for exploring the properties of IDPs as well as conformational switching events that are induced by ligand binding. Disordered regions undergo deuteration with k_{HDX} rate constants that approach k_{ch} , i.e., the value expected for unprotected amides.^{110,111} Accurate measurements of these rapid kinetics are challenging with conventional HDX/MS technology. The application of customized rapid mixing devices is an elegant solution to this problem.^{112,113} Another approach is to exploit the pD dependence of k_{ch} (eq 3) for slowing down the deuteration kinetics.^{64,65}

Membrane Protein HDX/MS. IMP studies remain highly challenging, but in recent years a number of research groups have begun to tackle this issue by HDX/MS. Owing to their extreme hydrophobicity, many IMPs are difficult to digest under typical quench conditions. Also, LC/MS analysis of the

resulting peptides can be problematic. HDX/MS studies on IMPs are most commonly conducted on detergent-solubilized species.^{107,114,115} A small number of investigations were successful in characterizing the deuteration behavior of IMPs in a membrane environment. It was demonstrated that the results obtained in this way can be markedly different from those seen for solubilized proteins.^{116,117} Clearly, the further development of robust strategies for interrogating the function, dynamics, and interactions of IMPs in their native bilayer would be a huge step forward.

Pulsed HDX/MS. All the HDX/MS experiments discussed above were conducted under continuous-labeling conditions, where the protein of interest is exposed to D₂O for various time intervals prior to mass analysis. Those studies serve to characterize the structure and dynamics under *equilibrium* conditions. In contrast, pulsed HDX studies are an essential tool for exploring protein conformational changes in non-equilibrium *kinetic* experiments. The most widely used application of pulsed HDX/MS is the elucidation of protein

folding pathways and the structural characterization of short-lived folding intermediates. Owing to the rapid time scale of many folding reactions, many of these experiments require rapid mixing devices,¹¹⁸ although some proteins fold slow enough to permit the application of manual mixing.^{119,120}

The general workflow of pulsed HDX/MS experiments involves three sequential mixing events (Figure 3A). Mixer 1 exposes the initially denatured protein to refolding buffer, triggering the folding reaction via denaturant dilution. After a variable folding time interval, the protein is exposed to a brief labeling pulse at relatively high pH (at mixer 2) to ensure deuteration of protein regions that remain unfolded. Importantly, the extent of labeling will be lower in regions that already acquired stable structure by the time the labeling pulse is applied. The labeling pulse is terminated by acid quenching at mixer 3 after a short (but constant) interval, e.g., 10 ms. The capability to modulate the rate constant k_{ch} via changes in pH or pD (eq 3) is an important prerequisite for successful pulsed HDX experiments. The quenched samples can then be analyzed as described above for continuous-labeling studies. The level of structural information that can be extracted from pulsed HDX/MS studies is impressive, as recently demonstrated in experiments on ribonuclease H1.¹²¹ Refolding of the urea-denatured protein goes to completion within ~1 min. Analysis of the kinetic data reveals a linear folding pathway that involves the sequential assembly of four distinct folding units or “foldons” (Figure 3B–D).

Cytotoxic Protein Aggregates Studied by HDX/MS.

Misfolded proteins or protein degradation products can undergo aggregation, resulting in the formation of cytotoxic assemblies that have been implicated in Alzheimer’s, Parkinson’s, and other neurodegenerative disorders. Earlier work in this field has focused mainly on large amyloid fibrils that often represent the end point of aggregation. However, it has now become clear that much smaller soluble oligomers likely represent the actual cytotoxic species.¹²² Characterization of these oligomers remains difficult because of their considerable heterogeneity which tends to result in multimodal mass distributions after HDX.^{123–125} The most thoroughly studied systems in this context are $\text{A}\beta(1\text{-}40)$ and $\text{A}\beta(1\text{-}42)$, which represent proteolytic degradation products of the amyloid precursor protein APP.¹²⁶ A combination of HDX/MS, NMR spectroscopy, and optical measurements has been applied to explore how the structure and dynamics of APP affect the product ratio of the different $\text{A}\beta$ species.¹²⁷ Pulsed HDX studies suggest that the formation of $\text{A}\beta$ oligomers proceeds in a self-catalyzed fashion, where the center region of the polypeptide chains interact first, followed by the formation of contacts in the C and N terminal regions.¹²⁰ The deuteration pattern of $\text{A}\beta(1\text{-}42)$ oligomers is consistent with a β -turn- β motif similar to that proposed for mature amyloid fibrils.¹²⁴ Oligomeric $\text{A}\beta(1\text{-}40)$ likely forms a β -barrel structure.¹²⁵ HDX/MS was also applied to study the conversion of the prion protein PrP^{C} to its cytotoxic PrP^{Sc} form.^{125,126} The data obtained in this way are consistent with a large-scale conformational switch from the monomeric α -helix-rich PrP^{C} conformation to an aggregated PrP^{Sc} structure that is dominated by β -strands.^{128,129}

Application of HDX/MS to Protein Therapeutics.

Protein drugs are subject to proteolytic degradation once they have entered the body. One way to enhance the lifetime of these species is via conjugation with synthetic polymers such as poly(ethylene glycol) (PEG). PEGylation poses significant

analytical challenges because it introduces a high level of heterogeneity, resulting in extremely complex mass spectra. This effect is due to the variability in the polymer chain lengths, differences in the number of chains per protein molecules, and differences in the attachment sites.¹³⁰ Similar problems are encountered with glycosylated protein drugs.⁵³ Despite these challenges, HDX/MS is rapidly establishing itself as a key tool in this area.⁵⁰ Comparability studies are one important application, where HDX/MS is used to confirm the batch-to-batch consistency of a protein drug or for studying the effects of PEGylation.⁹⁷ Another field of interest is epitope mapping for understanding the interaction of monoclonal antibodies with their targets.¹³¹ As noted above, the results of such binding studies have to be interpreted with caution because allosteric effects have to be taken into account.^{49,96} A simplistic analysis of binding data in terms of solvent occlusion may therefore be misleading.⁵⁰

Single Amide Resolution. Traditional HDX/MS experiments yield deuteration data at the peptide level, i.e., typically with a spatial resolution of ~10 residues. It is desirable to enhance this spatial resolution, ultimately down to the single residue level. Practitioners interested in such single residue HDX data can choose between three approaches. (1) HDX/NMR measurements have been a reality for more than 25 years,¹³² and they continue to be a key tool for structural biology investigations.¹³³ In contrast to digestion-based HDX/MS, however, the application of NMR methods to large biomolecular systems remains difficult. (2) Electron-based fragmentation methods allow an extension of HDX/MS into the single-residue regime, as discussed in the subsequent section. (3) Overlapping peptides can potentially be used to generate single residue data on the basis of subtractive analyses.^{70,121,134,135} For example, the difference in deuteration levels for peptides 1–10 and 1–11 should reveal the deuteration extent of residue 11. For this purpose it is necessary to generate digests with many overlapping peptides,¹³⁶ possibly via the use of complementary proteases.^{93,94} It has been pointed out, however, that the occurrence of differential back exchange for overlapping peptides can potentially introduce systematic errors into single-site HDX information obtained via subtractive analyses.⁸⁸

HDX/MS with Electron-Based Fragmentation. While most HDX/MS investigations achieve spatial resolution via solution phase digestion, there is also the option of following a top-down approach that employs the fragmentation of intact proteins in the vacuum of the mass spectrometer.⁴⁶ Early work in this area was based on CID which produces a series of b and y ions. It has now been recognized that collisional activation tends to induce H/D migration along the polypeptide backbone (“scrambling”), thereby randomizing the exchange pattern.¹³⁷ In contrast, ECD and ETD allow top-down experiments to be conducted without any significant scrambling.^{46,138,139} The backbone amide deuteration status can be obtained by subtractive analysis of consecutive c and z[•] ions, similar to the strategy outlined above for solution phase digestion data.^{70,88} Often the N- and C-terminal fragment ion series overlap, providing an internal consistency check of the deuteration data obtained. The nonspecific nature of electron-based dissociation provides excellent sequence coverage. While top-down HDX/MS does not always provide single-residue information, an average resolution of ~2 residues has been demonstrated for proteins as large as 29 kDa.¹⁴⁰ This significantly surpasses the spatial resolution typically obtained

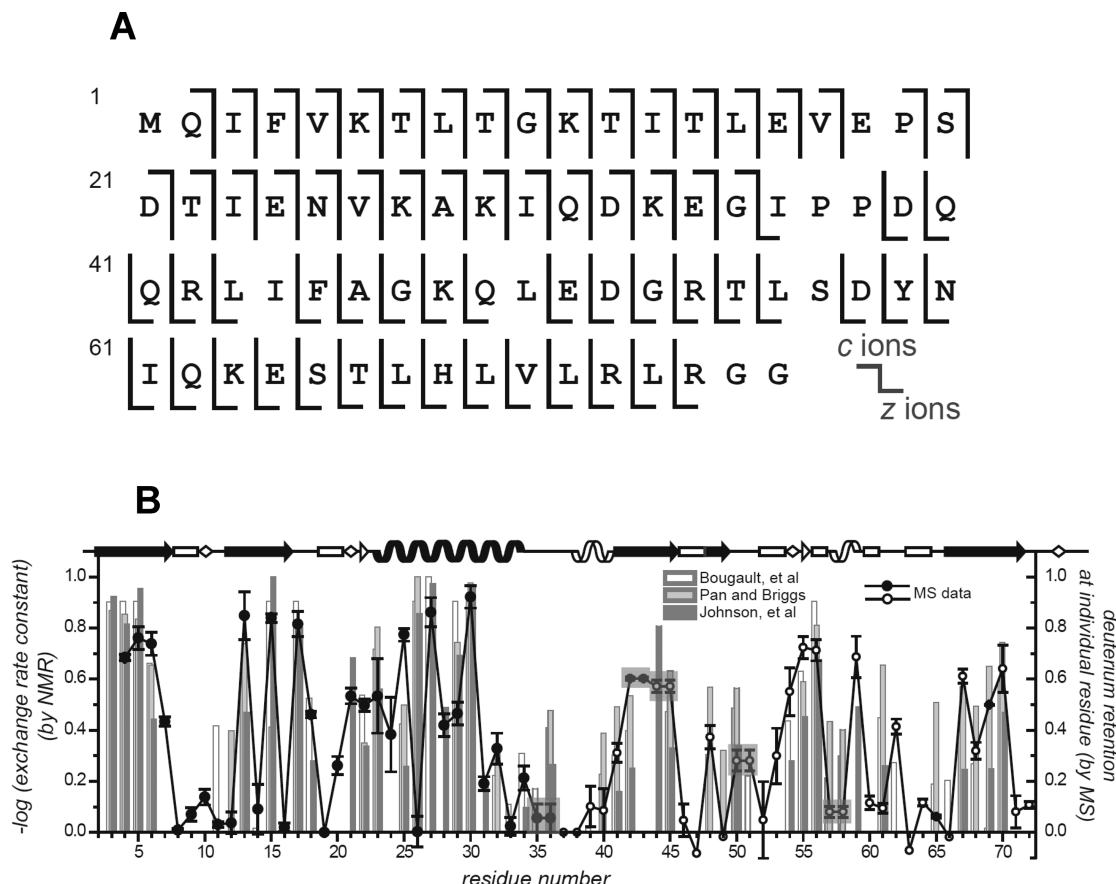


Figure 4. Structure and dynamics of native ubiquitin (76 residues) monitored by top-down ECD HDX/MS. (A) Cleavage map, showing c and z^{*} fragment ions. (B) HDX protection pattern determined by top-down HDX/MS (line-graph; closed symbols, c ions; open symbol, z^{*} ions). For comparison, the bar graphs depict protection data from three different HDX/NMR studies. Secondary structural elements are shown along the top of panel B. Reprinted with permission from ref 142. Copyright 2013 National Academy of Sciences of the United States of America.

in proteolysis experiments.^{85,141} For smaller proteins, single residue resolution can be obtained for most backbone amides (Figure 4).¹⁴² Interestingly, top-down HDX/MS can also be conducted via MALDI in-source decay, which produces a consecutive c ion series comparable to ECD and ETD.¹⁴³

What is the better method, bottom-up or top-down HDX? This question must be answered on a case-by-case basis. The acquisition of high quality top-down spectra, as well as the interpretation of these data, becomes increasingly challenging as protein size increases. The upper mass limit amenable to top-down HDX is currently in the range of ~30 kDa, i.e., comparable to that of HDX/NMR. Ongoing improvements in resolution and sensitivity of Fourier transform mass analyzers will likely expand the protein size range amenable to top down HDX/MS in the near future.¹⁴⁴

A key advantage of top-down HDX/MS is the possibility to interrogate *specific protein conformers* in structurally heterogeneous samples. There are many scenarios that involve coexisting conformational species, for example, in the context of protein folding and aggregation.^{12,13,15,16} Most existing analytical techniques can only characterize such samples in a population-averaged fashion, such that detailed insights on the properties of individually species cannot be obtained. The capability of top-down HDX/MS to overcome this limitation was first demonstrated in investigations on neurotoxic A β aggregates.^{124,125} Prerequisite for the successful application of this strategy is an HDX labeling pattern that provides a bimodal

(or multimodal) mass distribution, such that quadrupole precursor selection can be used to filter out a specific subset of ions which is then subjected to dissociation and mass analysis. Such conditions can be implemented in kinetic folding experiments that employ pulsed HDX (as discussed above).¹¹⁸ Under continuous labeling conditions, multimodal mass distributions are only observable in the EX1 regime, where two or more conformers interconvert on a time scale that is slower than k_{ch}^{-1} . This concept has recently been applied for characterizing the structural properties of a ubiquitin intermediate under various solvent conditions.¹⁴²

In addition to top-down HDX/MS, it is also possible to use electron-based fragmentation to enhance the spatial resolution of solution phase digestion experiments. Such investigations are conducted by subjecting the peptic peptides to ETD or ECD as they elute from the LC column.^{145,146} It is also possible to bypass the LC step and to conduct the analysis in a continuous-flow system.¹⁰⁶ Such hybrid approaches of solution phase digestion and gas phase fragmentation can provide single residue resolution. When applying this approach one has to keep in mind that hydrolysis converts the amide N–H (or N–D) group of the first peptide residue into an amine that will undergo complete back exchange. In addition, the backbone amide of residue 2 in the peptide will undergo back exchange as well. In other words, each proteolytic cleavage leads to information loss at two amide linkages.⁴⁹ This implies that

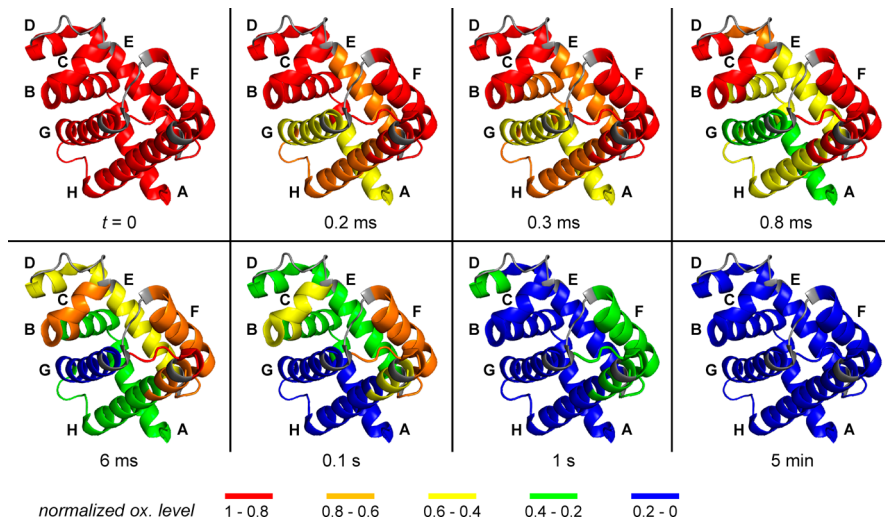


Figure 5. Structural changes during apo-myoglobin folding as measured by pulsed $\bullet\text{OH}$ labeling (FPOP) at different time points following a submillisecond mixing step. Normalized oxidation levels were mapped onto the crystal structure of the native protein using a five-level color code. Red corresponds to regions that are labeled to a similar extent as in the $t = 0$ unfolded reference; blue represents segments that have a solvent accessibility similar to that of the $t = 5$ min native structure. Helices A and G are among the first to fold, followed by H. The resulting AGH intermediate is fully established after 0.1 s. Reprinted from ref 174. Copyright 2013 American Chemical Society.

ETD or ECD analysis of relatively large peptides (i.e., a middle-down approach) should provide the most accurate information.

■ COVALENT LABELING

General Considerations. Covalent labeling (also known as “footprinting”) techniques are conceptually related to HDX because both approaches exploit reactivity differences in various parts of a protein to uncover conformational information. As noted above, HDX primarily monitors protein structure of dynamics at the secondary structure level by probing the reactivity of amide backbone sites. In contrast, covalent labeling techniques provide insights into the solvent accessibility of side chains. Exposed regions can react with a covalent probe, whereas burial due to binding interactions or conformational changes leads to protection.¹⁴⁷ Covalent labeling, therefore, provides information that is complementary to data obtained by HDX methods.^{115,148–150} The application of covalent labeling to nucleic acids has been demonstrated as well.^{10,151}

It might be argued that HDX also represents a covalent labeling technique, since N–H and N–D bonds represent covalent linkages. However, from a practical perspective there is a big difference between the two techniques. As discussed above, backbone deuterium is a fleeting moiety that tends to undergo rapid back exchange.⁸⁸ Collisional activation induces H/D scrambling.^{46,138} In contrast, covalent labeling agents result in side chain modifications that are highly stable during sample handling, a fact that is beneficial for analyses by bottom-up peptide mapping¹⁴⁷ or top-down MS.^{152,153} Scrambling of the label as a result ion activation is of no concern, although hidden complexities associated with some agents can occasionally lead to unexpected results.¹⁴⁸ An interesting new twist is the application of tagging agents that are UV absorbing, thus permitting the specific photodissociation of labeled peptides.¹⁵⁴ Another clever strategy is the use of isotope-coded affinity tag (ICAT) reagents, a strategy that allows the enrichment of covalently labeled peptides.¹⁵⁵

While the permanent nature of covalent labels simplifies some aspects of the workflow, there are also a number of complicating factors. In contrast to HDX experiments,

differentially labeled peptides do not coelute during LC, a fact that complicates the analysis under conditions where multiple products are formed. Also, covalent tagging of enzymatic recognition sites may alter proteolytic cleavage patterns in bottom-up studies. A general concern is that the introduction of covalent modification(s) can alter the protein structure. This last issue is usually addressed by keeping the number of covalent modifications per protein relatively low. Kinetic measurements represent a useful tool for confirming the absence of undesired labeling-induced conformational changes. Such control experiments tend to be time-consuming, but this issue may be overcome in multiplexed studies employing isotopically encoded reagents.¹⁵⁶ Similar approaches have been employed for probing protein stability and binding in thermodynamic measurements.¹⁵⁷

Covalent labeling techniques have been successfully applied for exploring the structure and interactions of biomolecular analytes for many years. A wide range of chemical probes is available,¹⁴⁷ and sometimes the application of more than one type of labeling chemistry is advisable for addressing a specific problem.¹⁵⁸ Interesting biological applications continue to emerge,^{152,159} but from an analytical perspective this field has experienced only modest growth over the past 2 years. A notable exception is the area of hydroxyl radical ($\bullet\text{OH}$) labeling, which has attracted considerable recent attention.

Hydroxyl Radical Labeling. $\bullet\text{OH}$ is a highly reactive species that generates oxidative modifications at solvent-exposed side chains. The fairly nonselective nature of $\bullet\text{OH}$ allows solvent accessibility studies on different types of residues simultaneously. Sulfur-containing residues react most readily, followed by aromatic and aliphatic side chains. $\bullet\text{OH}$ can be produced by various methods, including synchrotron radiolysis,¹⁶⁰ γ -irradiation,¹⁶¹ pulsed electron beams,¹⁶² and electrochemical flow cells.¹⁶³ Another interesting approach is $\bullet\text{OH}$ production by UV laser photolysis of dilute H_2O_2 inside a continuous-flow capillary tube, a technique that is often referred to as fast photochemical oxidation of proteins (FPOP).¹⁶⁴

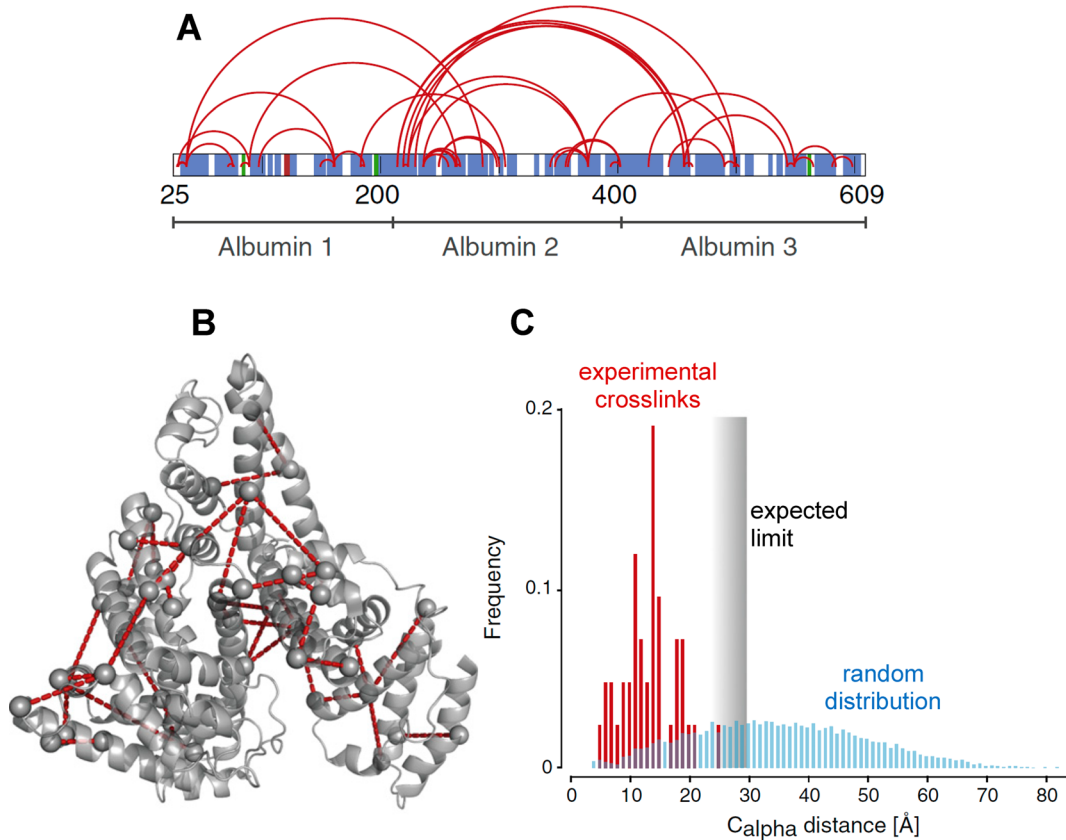


Figure 6. Cross-linking data obtained for human serum albumin (HSA), a protein that has three distinct domains. The experiments were conducted using bis[sulfosuccinimidyl] suberate (BS3), which cross-links the ϵ -amino groups of Lys side chains. (A) Mapping of MS-detected cross-links (red) to the HSA sequence. (B) Mapping of the cross-links to the crystal structure of HSA. (C) Diagram comparing the C_{α} distance distribution of MS-detected cross-links (red) and a theoretical random distribution that considers all possible Lys residues. The expected limit of the allowed distances (25 – 30 Å) is given by the length of the cross-link spacer plus two times the length of a Lys side chain. None of the detected cross-links fall outside this allowed range. Reprinted with permission from ref 178. Copyright 2013 Elsevier.

Quantitative analyses of the oxidation patterns are traditionally conducted at the peptide level, by subjecting the protein to a bottom-up approach after labeling. A number of groups have now proposed improved LC–MS/MS approaches aimed at providing labeling levels with single residue resolution.^{165–168}

Because solvent accessibility is a primary determinant of $^{\bullet}\text{OH}$ labeling, this technique is well suited for monitoring protein–protein interactions,¹⁶⁹ for example, in the context of epitope mapping studies.¹⁷⁰ This approach can also be applied to protein–DNA complexes,¹⁶¹ IMP binding studies,¹¹⁴ and even for *in vivo* experiments.¹⁷¹ For IMPs of unknown structure $^{\bullet}\text{OH}$ labeling data can provide valuable constraints for validating the results of computer-generated topology maps.¹⁷² In future work it should be possible to employ such experimental data to guide the prediction of high-resolution IMP conformational models.

One of the most remarkable features of $^{\bullet}\text{OH}$ labeling is the extremely rapid time scale of the labeling step. It has been estimated that under properly optimized FPOP conditions, side chain oxidation occurs within $\sim 1 \mu\text{s}$. This short time scale implies that protein covalent modifications are introduced on a time scale that is faster than most conformational changes. Thus, FPOP should be largely immune to structural distortion events that can be encountered with other covalent modification techniques.¹⁷³ Another notable implication is that FPOP is predestined for pulsed labeling studies that provide insights into structural features of short-lived folding

intermediates. We already introduced such time-resolved studies in a HDX context (Figure 3). One of the problems with pulsed HDX is the highly basic pH (or pD) required during labeling which can interfere with the folding process. In contrast, FPOP allows the ultrarapid labeling of proteins under neutral conditions. One of the long-standing problems in biophysical chemistry is the characterization of the very earliest folding steps, i.e., the submillisecond range. Past studies in this area were largely based on optical techniques that have a superb time resolution but that do not provide a lot of structural information. The combination of FPOP with an ultrarapid folding trigger provides the opportunity to gain unprecedented insights into these very early conformational changes. One trigger technique that is suitable for this purpose includes a laser-based temperature jump for the refolding of cold-denatured proteins.¹⁶⁴ Ultrarapid mixing provides another approach for folding studies via a pH jump or a denaturant dilution step. This concept has recently been demonstrated in submillisecond folding experiments on apo-myoglobin (Figure 5).¹⁷⁴ Carbene-based covalent labeling approaches might provide an alternative avenue for investigating ultrarapid conformational changes.^{168,175} The use of laser-based triggers other than temperature jumps would further expand the scope of such experiments.¹⁷⁶

■ COVALENT CROSS-LINKING

Similar to the labeling approaches discussed in the previous chapter, chemical cross-linking also relies on the introduction of covalent modifications. The key difference is that cross-linking involves the use of *bifunctional* reactive probes. The technique is based on the principle that two protein side chains that are separated by a certain distance will undergo coupling when exposed to a cross-linking agent of the appropriate length. Analogous techniques can be applied to nucleic acids¹⁰ and protein/nucleic acid complexes.¹⁷⁷ The detection of cross-links by MS provides low resolution information on the structure of a macromolecular analyte or the spatial arrangement of subunits in a complex. The principle underlying this technique is illustrated in Figure 6.¹⁷⁸

A large number of cross-linkers has been developed over the years. A detailed discussion of the underlying chemistry and reaction mechanisms is beyond the scope of our discussion (for recent reviews see refs 179–183; novices will find the article by Leitner et al.¹⁸⁴ particularly helpful). Most cross-linking agents have an architecture that comprises two reactive sites that are connected by a spacer. Lys side chains are the most widely used cross-linking targets, but Cys and other residues can also be used. One can distinguish homobifunctional reagents (e.g., for probing Lys~Lys distances) and heterobifunctional species (e.g., for introducing Lys~Cys linkages). Various spacer lengths can be used to explore different distance regimes. The presence of a homobifunctional cross-link implies that the C_{α} atoms of the corresponding residues are separated by a maximum distance of approximately (spacer length) + 2 × (side chain length).¹⁷⁸ The flexible nature of the covalent bridge connecting the two C_{α} atoms implies that there is no firm lower limit for the allowed distance. Thus, the information content of a cross-linking experiment generally decreases with increasing spacer length, especially when targeting Lys which has a very long side chain.¹⁸⁵ “Zero length” cross-linkers connect two side chains without introducing any additional atoms. For example, certain carbodiimides are capable of linking Lys and Asp or Glu via an amide bond.¹⁸⁴ Formaldehyde is a quasi-zero length cross-linker that couples two residues via a methylene bridge. The specificity of formaldehyde is low; Lys is the main target but other residues are reactive as well.¹⁸⁶ An interesting opportunity is the existence of large clinical repositories of formaldehyde-fixed tissue samples that could represent a rich source of information for protein interaction studies in health and disease.¹⁸⁷ Genetically encoded photoamino acids that undergo cross-linking after light exposure are a notable new development that will likely find widespread use in the near future.^{188,189}

Almost without exception, the workflow of cross-linking experiments is based on a tryptic digestion bottom-up approach. Analyzing the resulting spectra is a daunting task because one has to identify structurally informative cross-linked segments out of a very large number of unmodified peptides (the proverbial needle in the haystack!). The application of Fourier transform mass analyzers with extremely high resolution and mass accuracy is beneficial in this context. The situation is most challenging in protein interaction studies because here the cross-linking agent can react in four different ways:¹⁸⁴ (i) Dead-end products are formed when the cross-linker reacts with only one of its terminal groups. (ii) Intrapeptide connections originate from reaction of the cross-linker with side chains from the same protein that are close

together in sequence. (iii) Intraprotein links connect two tryptic peptides that originate from the same protein. (iv) Interprotein connections arise when the cross-linker reacts with two different protein subunits. Only the last type of cross-link carries information on protein–protein interactions. Different approaches have been introduced to cope with these challenges. For example, the use of isotopically labeled reagents results in specific peak patterns that are relatively easy to identify. CID-cleavable cross-linkers can generate easily recognizable peak patterns as well.¹⁹⁰ The inclusion of affinity tags for enrichment of cross-linker-containing digestion products is another commonly used strategy.^{178,183} Increasingly sophisticated software tools are becoming available to address the data analysis challenges encountered with these and other cross-linking strategies.^{191,192} In addition, the use of cross-linking data as distance restraints for computer-based modeling studies is rapidly gaining traction.^{185,193,194}

Cross-linking-based interaction studies can be conducted on purified proteins and protein mixtures. A wider net is cast by using tandem affinity purification of complexes from cell extracts.¹⁹⁴ Perhaps the most exciting prospect is the application of cross-linking studies *in vivo*.^{181,195} Such *in vivo* investigations can overcome the problem that protein–protein interactions may not survive the cell lysis and sample preparation steps that are inherent to *in vitro* protocols.¹⁹⁶ An obvious challenge with such cross-linking studies is that the bifunctional reagents have to be able to penetrate into subcellular compartments without causing major physiological perturbations.¹⁸¹ Because of its favorable solubility characteristics, formaldehyde is a surprisingly effective reagent in this regard.¹⁸⁶

■ ESI CHARGE STATE DISTRIBUTIONS

In positive ion mode ESI generates multiply protonated $[M + zH]^{z+}$ analyte ions where the number z of protons can cover a wide range. In the case of proteins, the appearance of the mass spectrum can be modulated by a number of factors,³² but the charge state distribution is chiefly determined by the solution phase conformation of the polypeptide chain.¹⁹⁷ Compact conformers give rise to narrow distributions of low protonation states, whereas unfolded structures generate wide distributions of ions that are much more highly charged. Hence, ESI charge state distributions have become a widely used tool for monitoring conformational changes of proteins in solution.^{7,20,198–200} The physical basis underlying the relationship between charge states and structure has remained nebulous over the past 2 decades.²⁰¹ New insights into the final stages of the ESI process have now emerged that shed some light on the mechanistic basis of this intriguing phenomenon. ESI mechanisms have been reviewed recently,^{202,203} and we will only provide a brief summary here, along with a few updates.

ESI Mechanism for Folded Proteins. Many studies support the idea that proteins in compact globular structures follow the charged residue model (CRM, Figure 7A).^{203–205} The CRM envisions that gaseous protein ions are formed when aqueous nanodroplets containing a single analyte molecule evaporate to dryness. According to the Rayleigh equation²⁰³ the number of charges z_R on these vanishing droplets can be estimated as $z_R = (8\pi/e) (\epsilon_0 \gamma R^3)^{1/2}$ where R is the droplet radius, ϵ_0 is the vacuum permittivity, and γ is the surface tension. It is assumed that a major fraction of the droplet charge is transferred to the protein during the final stage of solvent evaporation.²⁰² This CRM/Rayleigh model can account

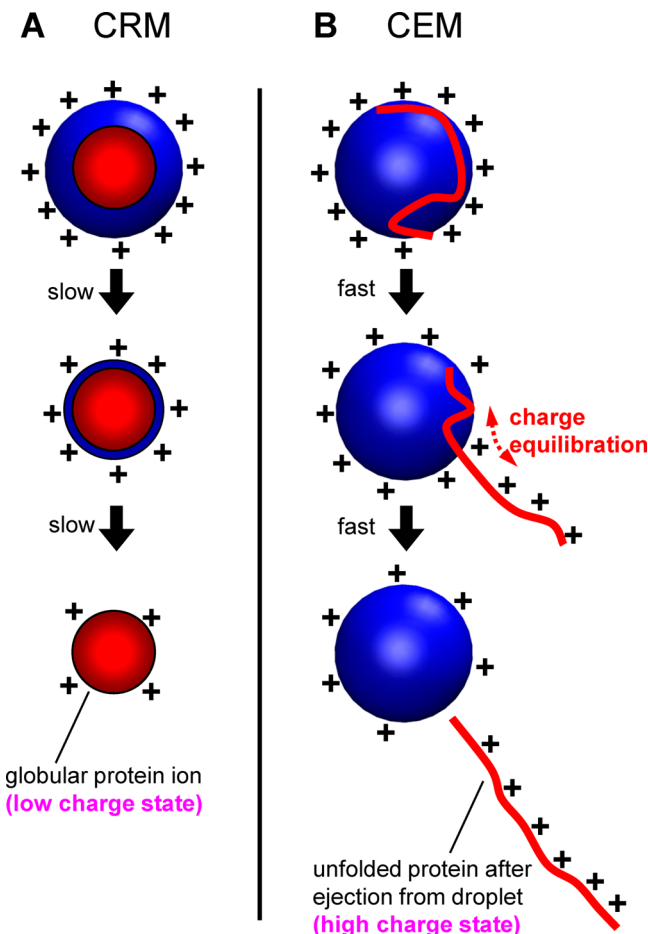


Figure 7. Cartoon representations of the final stages of protein ESI. The ESI droplet is depicted in blue, the protein is shown in red. (A) Folded proteins are expected to follow the charged residue model (CRM). (B) The chain ejection model (CEM) has been proposed for unfolded proteins. Further details are discussed in the text. Modified from ref 202. Copyright 2013 American Chemical Society.

for the experimental observation that the number of charges on a globular protein ion is close to z_R of a protein-sized water droplet.²⁰⁵ The CRM has been further advanced in recent years by proposing that the final charge state of a protein ion may be modulated by the field emission of low MW ions during droplet shrinkage.^{206,207} A slightly different model envisions that the ESI charge states of folded proteins are governed primarily by their gas phase basicity.²⁰⁸ However, none of these recent refinements^{206–208} disputes the core feature of the CRM, i.e., the production of compact protein ions via evaporation of small solvent droplets to dryness.

CID of Multiprotein Complexes. Prior to discussing the ESI mechanism of unfolded proteins we have to take a brief detour. Electrosprayed protein complexes typically undergo “asymmetric charge partitioning” upon collisional activation. This process entails the ejection of a single subunit with a disproportionately high fraction of charge. For example, a tetrameric complex might dissociate according to $M_4^{20+} \rightarrow M_3^{10+} + M^{10+}$, ejecting a product ion that carries half the total charge but only a quarter of the mass. This phenomenon is due to the fact that collisional activation induces large-scale unfolding of a single subunit, prior to its separation from the complex.²⁰⁹ The high protonation state of the ejected monomer is caused by charge migration. Excess protons in

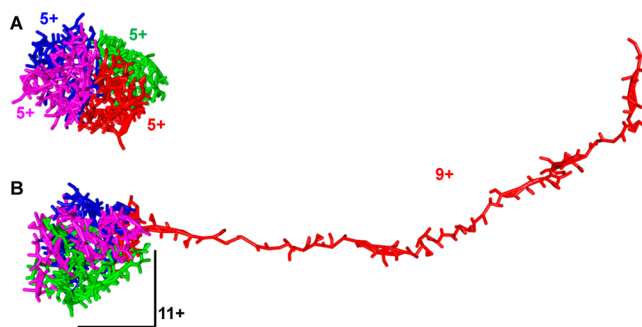


Figure 8. Molecular dynamics simulation results for the dissociation of a transthyretin M_4^{20+} ion during collisional activation in the gas phase. (A) Native structure of the tetramer where each subunit carries five charges. (B) Collisional activation causes one of the subunits (red) to unravel and accumulate additional charge. This subunit will ultimately depart as a highly charged ion. Modified from ref 211. Copyright 2013 American Chemical Society.

collisionally activated complexes are highly mobile and will adopt a spatial distribution that minimizes the electrostatic energy of the overall system. Coulombically driven proton migration to the unfolded subunit is therefore a highly favorable process. In this way the subunit accumulates significant charge, until it ultimately separates from the complex.²¹⁰ Molecular dynamics simulations employing a newly developed charge hopping algorithm have confirmed the occurrence of large-scale subunit unfolding with concomitant charge accumulation and subsequent ejection (Figure 8).²¹¹ Charge migration does not take place during surface-induced dissociation (SID), presumably because the short time scale of the process does not allow subunit unfolding prior to separation.²¹²

ESI Mechanism for Unfolded Proteins. Computational studies suggest that the ESI process for unfolded proteins proceeds via a mechanism that is very different from the CRM.^{202,213} The chain ejection model (CEM)²⁰² predicts that unfolded proteins emerge from the droplet surface in an extended conformation, driven by a combination of electrostatic repulsion and hydrophobicity (Figure 7B). This process occurs within nanoseconds, much faster than droplet evaporation to dryness which is the hallmark of the CRM. This different time regime may help explain why unfolded proteins tend to generate higher ESI-MS signal intensities than folded conformers. The CEM posits that charge equilibration between the droplet and its protruding polypeptide tail is responsible for the high protonation states of unfolded proteins. This charge migration is directly analogous to the asymmetric charge partitioning illustrated in Figure 8 for CID of a protein complex. Both processes involve the ejection of an extended chain that accumulates a high number of protons from a large globular parent moiety, and both take place under collisional activation. It has been noted that the gas phase fragmentation of a protein complex can produce ESI mass spectra that are very similar to those generated from an unfolded solution phase conformation.^{214,215} This similarity is no coincidence, since CID of protein complexes and the production of CEM ions basically share the same mechanism. Taken together, the CEM and the CRM provide a foundation for the relationship between protein structure and ESI charge state distribution. Folded proteins follow the CRM, forming ions in low charge states. Conversely, the high charge states seen for unfolded species are a direct result of the CEM. As discussed elsewhere,²⁰² the CEM can also account for the much

larger heterogeneity of the charge states that is generally seen for unfolded species.

“Supercharging” and Related Phenomena. The usefulness of ESI charge distributions for monitoring protein conformational changes is undisputed.^{7,20,198,199} However, recent work suggests that proteins may undergo conformational changes while they reside within the ESI droplet. This can give rise to disparities with the protein conformation in bulk solution.²¹⁶ Protein conformational alterations in the droplet phase might arise from environmental changes caused by differential solvent evaporation in the case of binary solvents.²¹⁷ This mode of action likely applies to certain “supercharging” agents²¹⁸ such as *m*-nitrobenzyl alcohol (*m*-NBA). These compounds, when added to a native protein solution in low concentration, lead to the formation of significantly elevated charge states. Preferential water evaporation increases the concentration of the supercharging agents during the lifetime of the ESI droplet, causing protein unfolding prior to gas phase ion formation.²¹⁹ Microbubbles resulting from bicarbonate outgassing also appear to cause unfolding inside the droplet, thereby triggering the formation of elevated ESI charge states.^{220,221} Overall, it appears that many “supercharging” agents act by causing protein denaturation in the ESI droplet. This results in a switch in the ESI mechanism from the CRM to the CEM. The latter generates much higher charge states, as discussed in the previous section. It has been suggested that ESI charge state distributions may also depend on the surface tension of the solvent,²²² but that view is not universally accepted.²²³ Another interesting way to modulate the ESI charge state distributions of proteins is by exposing the ESI plume to acidic or basic vapors.^{224–226} It is not always clear if the effects observed in such experiments are due to gas phase proton transfer, protein conformational changes within the ESI droplets, or a combination of both.

NATIVE MASS SPECTROMETRY AND ION MOBILITY SPECTROMETRY

The structural MS techniques discussed above do not make any assumptions regarding the conformation of biomolecular analytes after their release into the gas phase. In this section we focus on approaches that may be referred to as “native” MS, where the (partial) retention of solution phase structure and interactions is essential. Almost without exception^{227,228} the work in this area employs ESI or nanoESI. The solvent typically used is water with a low concentration of ammonium acetate at pH ~7. The volatile nature of this background electrolyte ($\text{NH}_4^+(\text{aq}) + \text{CH}_3\text{COO}^-(\text{aq}) \rightarrow \text{NH}_3(\text{g}) + \text{CH}_3\text{COOH}(\text{g})$) ensures that undesired adduct formation during ESI is minimized. Although commonly referred to as a “buffer”, the actual buffering capacity of ammonium acetate at neutral pH is negligible.²²⁰ The most widely used application of native MS is the characterization of protein–protein and protein–ligand complexes. Many researchers combine analyses of these noncovalent complexes with IMS, which is why we discuss both of these concepts in the same section (for earlier reviews see refs 200, 229–235).

Preservation of Native-Like Structures in the Gas Phase. Biological molecules have evolved in an aqueous environment, and interactions with water are an integral part of the factors that stabilize their active conformations. In particular, the hydrophobic effect is one of the dominant driving forces of protein folding.^{236,237} ESI entails complete desolvation as well as major changes in the protonation states

of titratable groups. It may seem counterintuitive that solution phase structure would survive under such conditions. Indeed, opinions on this topic are controversial as epitomized by the titles of two recent studies: “How Ubiquitin Unfolds after Transfer into the Gas Phase”⁴⁴ and “(...) Native Solution Structure of Ubiquitin Survives (...) in a Solvent-Free (...) Environment”.⁴³ It is undisputed that in some cases the transition from solution to the gas phase can alter and/or disrupt biomolecular structures and interactions.^{238–242} Nonetheless, evidence for the retention of native-like structures comes from the fact that noncovalent interactions as well as the overall size of the analytes can often be preserved in the gas phase. Overall, it appears that desolvated biomolecular ions can get trapped in local free energy minima. Under properly optimized conditions, these metastable states retain aspects of their solution phase structure, at least on the millisecond time scale of typical gas phase experiments.^{243–245}

One factor that determines whether or not solution structure gets retained is the ESI mechanism pursued by the analyte. Electrostatic stretching experienced by a CEM-generated ion will promote the breakdown of residual structure.²⁰² This view is consistent with the finding that electrosprayed semidenatured proteins do not retain a clear memory of their solution phase properties. Examples of such species include myoglobin folding intermediates²⁴⁴ and the ubiquitin A-state.⁴³ In contrast, the CRM represents a relatively gentle ionization mechanism that promotes the preservation of compact biomolecular structures.²⁴⁴ Small proteins may be most vulnerable to ESI-induced structural changes due to their relatively large surface-to-volume ratio. Large multiprotein assemblies often have a considerable fraction of their side chains engaged in inter- or intramolecular protein interactions, such that desolvation tends to have less dramatic structural consequences. Nonetheless, the dissociation of protein complexes during or after ESI as well as the occurrence of other types of structural changes is always possible.²⁴¹ Similar considerations apply to nucleic acid assemblies.²⁴²

The capability to maintain major aspects of biomolecular conformations and interactions during ESI opens the door to the field of “gas phase structural biology”.^{234,246} Critics of this area should consider that other well accepted methods such as cryo-EM⁵ and even X-ray crystallography⁴ also involve the characterization of biological analytes in a nonphysiological environment.

Ion Mobility Spectrometry and Other Techniques for Probing Gas Phase Structures. Part of the controversy regarding the properties of electrosprayed biomolecular systems stems from the fact that it is exceedingly difficult to determine gaseous structures with high resolution. Recent years have witnessed interesting attempts to transfer some of methodologies developed for solution measurements such as HDX,^{247–250} covalent labeling,^{251,252} cross-linking,²⁵³ and Förster resonance energy transfer (FRET)²⁵⁴ to the gas phase. Infrared multiphoton dissociation (IRMPD)^{255,256} and other types of action spectroscopy²⁵⁷ are a rich source of structural information for relatively small analytes, but their applicability to larger systems remains limited. ECD can provide protein structural information based on the idea that cleaved segments will only separate from each other if they are not linked by noncovalent bonds.²⁵⁸ Also, extended and/or unfolded regions tend to accumulate more of the ionic charge, thereby providing these segments with an elevated electron capture efficiency during top-down ECD.²⁵⁹

IMS represents the most widely used tool for characterizing the structures of biomolecular systems in the gas phase, typically with the implicit assumption that the data obtained are correlated with the analyte behavior in solution. In IMS ions are passed through a buffer gas under the influence of a weak electric field. The drift time t_d depends on Ω/z , where Ω is the rotationally averaged CCS which represents a measure of analyte size. Unfolded ions have larger Ω values than tightly folded conformers.²⁶⁰ In recent years IMS has been adopted by a very large user community due to the availability of commercial quadrupole-time-of-flight (Q-TOF) systems that allow IMS measurements via traveling-wave ion guides (TWIGs).²⁶¹ Operating these devices at cryogenic temperature offers the opportunity to study partially hydrated biomolecular ions.²⁶² The resolution ($\Omega/\Delta\Omega$) of TWIGs is relatively low, typically around 40.²⁶¹ Resolution values up to 1000 have been demonstrated in a cyclical drift tube instrument.²⁶³ Differential IMS (also known as field asymmetric waveform IMS, FAIMS) represent an alternative way of conducting high-resolution gas phase separations.²⁶⁴ Unfortunately, the relationship between analyte structure and FAIMS data remains poorly understood, limiting the applicability of this approach for conformational analyses.

On traditional drift tube devices, the conversion of measured t_d values to CCSs is straightforward. The situation is more complex when using TWIG systems, but calibration methods have been developed to address this issue.^{246,265,266} IMS data are typically analyzed on the basis of comparisons with theoretical CCSs that were calculated for known crystal structures or for computer-generated structural models. MOBCAL and related tools are widely used for this purpose.^{267–269} For small analytes, only relatively few gas phase structures are compatible with the measured CCSs.²⁷⁰ The situation becomes more ambiguous for larger systems because a given CCS may be compatible with a large number of candidate structures.²⁷¹ Recent work related to drag enhancement and other factors points to additional complications, i.e., large uncertainties (up to 40%) for existing $t_d-\Omega$ conversion methods.^{272–274} It may be advisable to conduct comparisons between measured and calculated CCSs only in a semi-quantitative fashion until this issue is resolved.

Protein–Protein Complexes. ESI Q-TOF (or ESI TOF) instruments remain the primary type of analyzer for the analysis of noncovalent protein complexes.^{275,276} Nonetheless, it is also possible to conduct such investigations on other platforms.²⁵⁹ One particularly impressive example is the detection of an 18 MDa virus capsid on an Orbitrap (Figure 9).²⁷⁷ The examination of viral particles by native MS/IMS represents one of many applications in this area.^{200,278,279} Various other types of protein assemblies have been studied using native MS,^{280,281} including cytotoxic aggregates,^{230,231,282,283} IMP complexes,^{284–287} and nanodisc-bound systems.^{288,289}

Given the delicate nature of many gaseous protein complexes, there is considerable interest in devising strategies that help stabilize these systems. Collisional activation during ion sampling is one of the main concerns, as this can induce dissociation via the unfolding mechanism discussed in the preceding chapter (Figure 8). A certain degree of collisional activation, however, is required to ensure adequate desolvation and adduct removal. ESI-MS based studies of noncovalent complexes therefore require a finely tuned set of acceleration voltages and gas pressures.^{266,285} The use of charge-reducing agents is one way to stabilize protein interactions in the gas

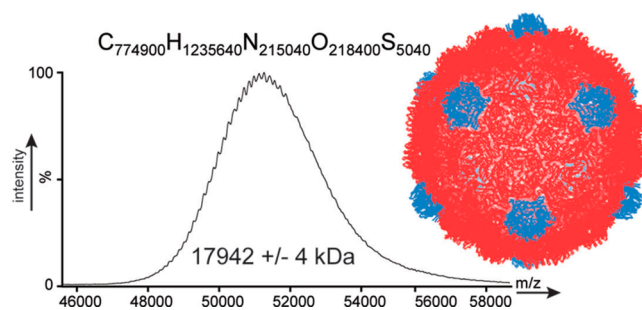


Figure 9. Detection of an intact virus capsid consisting of 420 identical subunits with a total mass of almost 18 MDa. The fine structure in the spectrum corresponds to resolved charge states that permit a reliable mass determination. Reprinted with permission from ref 277. Copyright 2013 Wiley.

phase,²⁹⁰ although charge reduction may be accompanied by conformational changes.²⁹¹ Stabilization may also be achieved by evaporative cooling. This phenomenon entails the loss of detergents or other low molecular weight species during collisional activation.^{292,293} Thus, the energy imparted to a partially desolvated macroion is dissipated via the disruption of protein–adduct interactions, instead of increasing the internal energy of the ion. The dissociation of anionic adducts A^- in the form of HA neutrals serves the same purpose.²⁹⁴ Bound cations can stabilize protein complexes either via a tethering mechanism or by reducing the availability of highly mobile charge carriers (protons) that would otherwise promote subunit unfolding via the mechanism of Figure 8.²⁹⁵

It is an intriguing question whether native MS/IMS can provide insights into the spatial arrangement of subunits within a multiprotein complex. As noted above, simple CCS measurements on intact complexes provide only limited information because there will be many different quaternary structures that would be compatible with a given CCS value.²⁷¹ More detailed insights can be obtained by focusing on the behavior of subcomplexes.^{232,296} This approach relies on two assumptions: (i) Slightly harsher experimental conditions will produce subcomplexes where tightly bound neighboring protomers remain attached to each other. The detection of such subcomplexes reports on the connectivity within the complex. (ii) The experimental conditions have to be chosen such that the overall structures of the subcomplexes (and hence their CCSs) resemble the situation in solution. CID is unsuitable for generating the intact subcomplexes required for this approach due to the prevalence of single chain ejection events that are accompanied by unfolding (Figure 8). SID shows more promise in generating subcomplexes that retain a native-like topology.^{215,297} At present the most successful approach for dissecting biomolecular assemblies into native-like subsystems is the use of mildly denaturing conditions in solution. IMS and connectivity data obtained in such studies provide restraints for the computer-generated models that can reproduce the overall topology of intact complexes with surprising accuracy (Figure 10).²⁹⁸

Other Types of Noncovalent Assemblies. Exploring interactions of proteins and other macromolecules with low MW binding partners is crucial for understanding ligand-induced conformational switching, drug action mechanisms, as well as enzyme allostery and inhibition.^{271,299–301} There is immense interest in developing robust strategies for the direct detection of the corresponding noncovalent complexes by

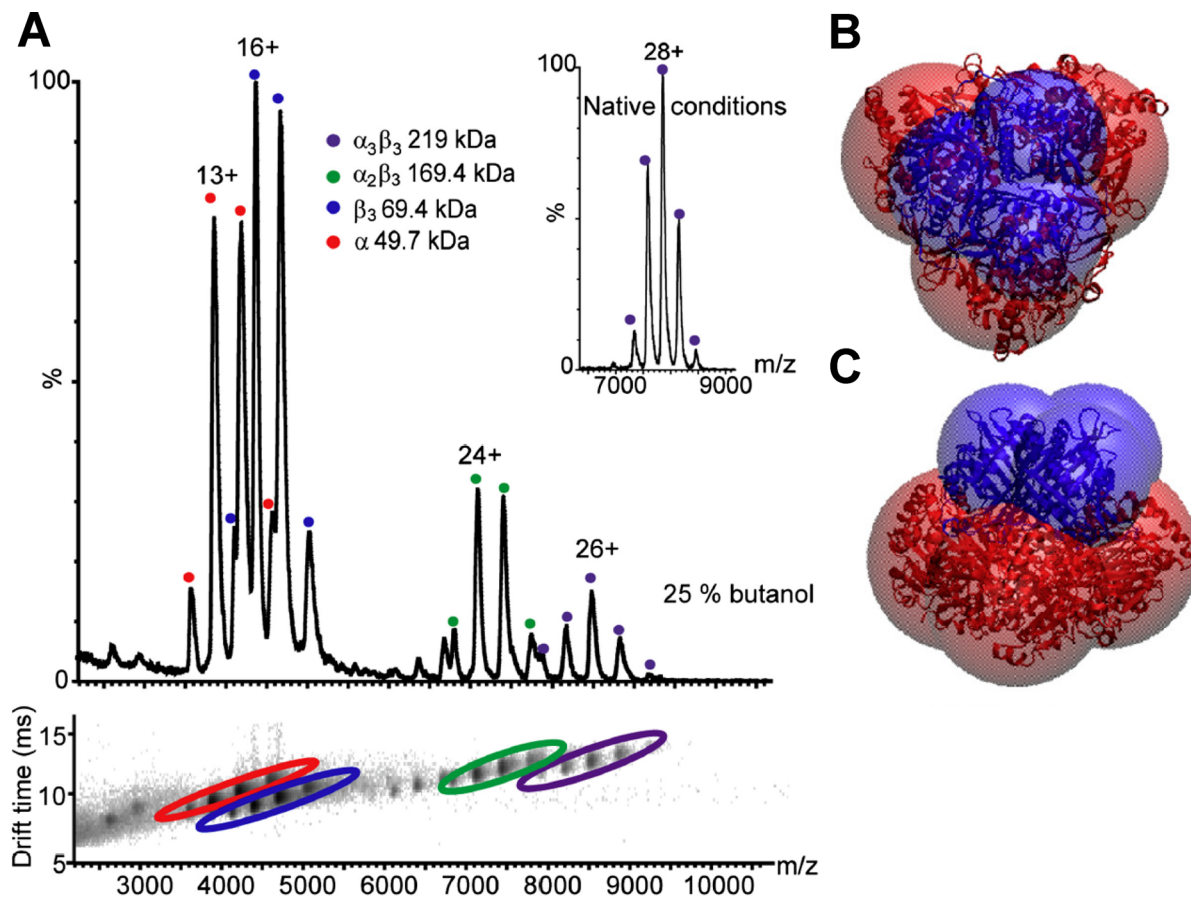


Figure 10. Low-resolution structure determination for nitrobenzene dioxygenase, a $\alpha_3\beta_3$ complex, using IMS of subcomplexes generated under mildly denaturing solution conditions. (A) Exposure to 25% butanol results in a mixture of intact complex in various charge states (purple) as well as subcomplexes $\alpha_2\beta_3$ (green), β_3 (blue), and free α (red). Shown along the bottom are the corresponding IMS drift time data. The inset shows the native spectrum acquired in aqueous ammonium acetate solution, in the absence of butanol. (B) Top view and (C) side view of a computational model generated based on these data are indicated using large spheres, superimposed on the actual X-ray structure. Reprinted with permission from ref 298. Copyright 2012 Elsevier.

native ESI-MS. The appeal of this approach lies in its simple mix-and-measure nature and in the short analysis time required. However, there still remains a number of technical hurdles.^{229,302} Key among these is the possibility that noncovalent interactions may not survive the transfer into the gas phase.³⁰³ Hydrophobically bound complexes tend to be most prone to dissociation,^{304,305} although there are now many examples where such complexes have been detected.^{293,306} Failure to observe some complexes may be due to the choice of solvent,³⁰⁷ keeping in mind that nonvolatile buffers and salts are incompatible with native ESI-MS. Conversely, the possibility exists that solutes associate nonspecifically with a macromolecule under CRM conditions as ESI droplets dry out.³⁰³ Thus, the direct ESI-MS approach for monitoring noncovalent interactions can suffer from false-positive and false-negative outcomes. Strategies to mitigate these problems include the use of reference proteins³⁰² and competition assays.³⁰⁸ “Catch-and-release” measurements involve the collisional dissociation of complexes to identify ligands in the case of poorly resolved analytes, such as nanodiscs³⁰⁹ or PEGylated protein drugs.

A comprehensive characterization of receptor–ligand interactions also comprises the measurement of the corresponding dissociation constants. In principle this can be accomplished on the basis of mass spectral peak intensity ratios.³⁰² Results obtained using this approach will be skewed under conditions

where in-source dissociation or ESI-mediated clustering occur.³⁰³ Also, free and bound forms of the receptor do not necessarily exhibit the same ionization efficiency.³¹⁰ The stability of noncovalent complexes in the gas phase can be assessed by CID methods. It is tempting to extrapolate the trends observed in these measurements to the solution phase. While this method seems viable for some systems,³¹¹ there generally does not seem to be a direct correlation between solution and gas phase stability.^{242,293}

Several attempts have been made to use top-down ECD for mapping the location of ligand binding sites on protein receptors. This approach requires the protein–ligand interactions to remain intact under conditions where the polypeptide backbone undergoes fragmentation. This method has shown considerable promise for electrostatically bound complexes.^{312,313} The use of supercharging agents in these experiments for enhancing the ECD efficiency can be dangerous as it often entails protein conformational changes (discussed above) that may alter the nature of the protein–ligand interactions.³¹⁴ Also, there is evidence for the possible occurrence of ligand migration in the gas phase.^{201,238,315,316} This last point brings us back to the fundamental issue raised at the outset of this chapter, i.e., the question to what extent solution phase structure is retained in the gas phase.

CONCLUDING REMARKS

Biological MS has come a long way since the inception of ESI²⁸ and MALDI²⁹ in the 1980s. Those ionization techniques first opened the door to relatively simple mass measurements on intact biomolecules. In the intervening years the field has matured to a point where structural MS provides detailed insights into biomolecular conformations, dynamics and interactions. MS-based methods will likely never replace existing structure determination tools such as X-ray crystallography, NMR spectroscopy, and cryo-EM. Instead, the impact of MS will be largest when used *in conjunction* with these and other classical tools. Practitioners should not limit themselves to just one type of structural MS technique. HDX, covalent labeling, cross-linking, charge state distributions, and native MS/IMS all yield complementary information.^{114,115,150,317,318} The old proverb that “the whole is greater than the sum of its parts” definitely rings true in this case.

The intriguing question to what extent solution phase structures of biological macromolecules can be retained in the gas phase will likely remain at the forefront of the field for the next few years. An exhilarating prospect in this context is the development of free electron lasers that might be capable of conducting high-resolution studies on individual gaseous molecules.³¹⁹ Also, the ongoing development of new ionization techniques³²⁰ and mass analyzers with ever increasing performance characteristics is certain to have a major impact.¹⁴⁴ By combining all of these experimental techniques with computational modeling and simulations it will be possible to generate a truly comprehensive picture of biological function in health and disease.

AUTHOR INFORMATION

Corresponding Author

*E-mail: konerman@uwo.ca. Phone: (519) 661-2111 ext. 86313.

Notes

The authors declare no competing financial interest.

Biographies

Lars Konermann is Professor of Chemistry and Canada Research Chair at The University of Western Ontario. He obtained his Ph.D. in Germany at the Max Planck Institute Mülheim/University of Düsseldorf) in 1996. This was followed by a postdoctoral fellowship at the University of British Columbia, Canada, from 1996 to 1998. The work of his group (<http://publish.uwo.ca/~konerman/>) focuses on the development and application of MS techniques for biological applications. Major areas include the use of HDX and covalent labeling for exploring protein structure and dynamics. In addition, the research group has a broad interest in MS fundamentals and biomolecular simulations.

Siavash Vahidi attended the National University of Iran, obtaining a B.Sc. in chemistry (2006–2010). He then moved to The University of Western Ontario to join the Konermann Laboratory to pursue a Ph.D. degree in biophysical mass spectrometry (2010 to present). His research interests span areas of protein structure, folding, and dynamics in the solution and in the gas phase.

Modupeola A. Sowole is a Ph.D. student at The University of Western Ontario in the Department of Chemistry under the supervision of Prof. Lars Konermann. She received her B.Sc. degree from the University of Lagos (Nigeria) in 2003. She then proceeded to obtain Master's degrees in Chemistry at both the University of Lagos and the University of Western Ontario. She joined the Konermann Lab in

2011. Her research focuses on the use of HDX/MS to probe protein structure and function.

ACKNOWLEDGMENTS

We thank Sarah Fegan from Prof. Mark Thachuk's laboratory for sending us coordinate files for Figure 8. Research conducted in the Konermann laboratory is funded by the Natural Sciences and Engineering Research Council of Canada (NSERC), the Canada Foundation for Innovation (CFI), the Canada Research Chairs Program, and The University of Western Ontario.

REFERENCES

- (1) Henzler-Wildman, K.; Kern, D. *Nature* **2007**, *450*, 964–972.
- (2) Robinson, C. V.; Sali, A.; Baumeister, W. *Nature* **2007**, *450*, 973–982.
- (3) Boehr, D. D.; Nussinov, R.; Wright, P. E. *Nat. Chem. Biol.* **2009**, *5*, 789–796.
- (4) Parker, M. W. *J. Biol. Phys.* **2003**, *29*, 341–362.
- (5) Milne, J. L. S.; Borgnia, M. J.; Bartesaghi, A.; Tran, E. E. H.; Earl, L. A.; Schauder, D. M.; Lengyel, J.; Pierson, J.; Patwardhan, A.; Subramaniam, S. *FEBS J.* **2013**, *280*, 28–45.
- (6) Mittermaier, A.; Kay, L. E. *Science* **2006**, *312*, 224–228.
- (7) Kaltashov, I. A.; Bobst, C. E.; Abzalimov, R. R. *Protein Sci.* **2013**, *22*, 530–544.
- (8) Nilsson, T.; Mann, M.; Aebersold, R.; Yates, J. R.; Bairoch, A.; Bergeron, J. J. M. *Nat. Methods* **2010**, *7*, 681–685.
- (9) Wintrode, P. *Biochim. Biophys. Acta: Proteins Proteomics* **2013**, *1834*, 1187–1187.
- (10) Fabris, D. *Anal. Chem.* **2011**, *83*, 5810–5816.
- (11) Han, L.; Costello, C. E. *Biochemistry (Moscow)* **2013**, *78*, 710–720.
- (12) Wolynes, P. G.; Eaton, W. A.; Fersht, A. R. *Proc. Natl. Acad. Sci. U.S.A.* **2012**, *109*, 17770–17771.
- (13) Wani, A. H.; Udgaoarkar, J. B. *Curr. Sci.* **2012**, *102*, 245–265.
- (14) Saibil, H. *Nat. Rev. Mol. Cell Biol.* **2013**, *14*, 630–642.
- (15) Prusiner, S. B. *Science* **2012**, *336*, 1511–1513.
- (16) Pastore, A.; Temussi, P. A. *Curr. Opin. Struct. Biol.* **2012**, *22*, 30–37.
- (17) Jucker, M.; Walker, L. C. *Nature* **2013**, *501*, 45–51.
- (18) Dyson, H. J.; Wright, P. E. *Nat. Rev. Mol. Cell Biol.* **2005**, *6*, 197–208.
- (19) Khan, H.; Cino, E. A.; Brickenden, A.; Fan, J. S.; Yang, D. W.; Choy, W. Y. *J. Mol. Biol.* **2013**, *425*, 1011–1027.
- (20) Beveridge, R.; Chappuis, Q.; MacPhee, C. E.; Barran, P. *Analyst* **2013**, *138*, 32–42.
- (21) Forman-Kay, J. D.; Mittag, T. *Structure* **2013**, *21*, 1492–1499.
- (22) Weiner, L. M.; Surana, R.; Wang, S. Z. *Nat. Rev. Immunol.* **2010**, *10*, 317–327.
- (23) Beckmann, N.; Kaltashov, I. A. *Adv. Drug Delivery Rev.* **2013**, *65*, 1001–1001.
- (24) Alley, S. C.; Anderson, K. E. *Curr. Opin. Chem. Biol.* **2013**, *17*, 406–411.
- (25) Kimchi-Sarfaty, C.; Schiller, T.; Hamasaki-Katagiri, N.; Khan, M. A.; Yanover, C.; Sauna, Z. E. *Trends Pharmacol. Sci.* **2013**, *34*, 534–548.
- (26) Whitelegge, J. P. *Anal. Chem.* **2013**, *85*, 2558–2568.
- (27) Katritch, V.; Cherezov, V.; Stevens, R. C. *Trends Pharmacol. Sci.* **2012**, *33*, 17–27.
- (28) Fenn, J. B. *Angew. Chem., Int. Ed.* **2003**, *42*, 3871–3894.
- (29) Karas, M.; Hillenkamp, F. *Anal. Chem.* **1988**, *60*, 2299–2301.
- (30) Chaurand, P. *J. Proteomics* **2012**, *75*, 4883–4892.
- (31) Inutan, E. D.; Wager-Miller, J.; Mackie, K.; Trimpin, S. *Anal. Chem.* **2012**, *84*, 9079–9084.
- (32) Yuill, E. M.; Sa, N.; Ray, S. J.; Hieftje, G. M.; Baker, L. A. *Anal. Chem.* **2013**, *85*, 8498–8502.
- (33) Paizs, B.; Suhai, S. *Mass Spectrom. Rev.* **2005**, *24*, 508–548.

- (34) Zubarev, R. A.; Zubarev, A. R.; Savitski, M. M. *J. Am. Soc. Mass Spectrom.* **2008**, *19*, 753–761.
- (35) Coon, J. J. *Anal. Chem.* **2009**, *81*, 3208–3215.
- (36) Zhurov, K. O.; Fornelli, L.; Wodrich, M. D.; Laskay, U. A.; Tsybin, Y. O. *Chem. Soc. Rev.* **2013**, *42*, 5014–5030.
- (37) Olsen, J. V.; Ong, S.; Mann, M. *Mol. Cell. Proteomics* **2004**, *3*, 608–614.
- (38) Zhou, H.; Ning, Z.; Starr, A. E.; Abu-Farha, M.; Figeys, D. *Anal. Chem.* **2012**, *84*, 720–734.
- (39) Fabris, D.; Kellersberger, K. A.; Wilhide, J. A. *Int. J. Mass Spectrom.* **2012**, *312*, 155–162.
- (40) Shaw, J. B.; Li, W.; Holden, D. D.; Zhang, Y.; Griep-Raming, J.; Fellers, R. T.; Early, B. P.; Thomas, P. M.; Kelleher, N. L.; Brodbelt, J. S. *J. Am. Chem. Soc.* **2013**, *135*, 12646–12651.
- (41) Wu, C.; Tran, J. C.; Zamdborg, L.; Durbin, K. R.; Li, M. X.; Ahlf, D. R.; Early, B. P.; Thomas, P. M.; Sweedler, J. V.; Kelleher, N. L. *Nat. Methods* **2012**, *9*, 822.
- (42) Ben-Nissan, G.; Sharon, M. *Chem. Soc. Rev.* **2011**, *40*, 3627–3637.
- (43) Wyttenbach, T.; Bowers, M. T. *J. Phys. Chem. B* **2011**, *115*, 12266–12275.
- (44) Skinner, O. S.; McLafferty, F. W.; Breuker, K. *J. Am. Soc. Mass Spectrom.* **2012**, *23*, 1011–1014.
- (45) Jaswal, S. S. *Biochim. Biophys. Acta* **2013**, *1834*, 1188–1201.
- (46) Konermann, L.; Pan, J.; Liu, Y. *Chem. Soc. Rev.* **2011**, *40*, 1224–1234.
- (47) Iacob, R. E.; Engen, J. R. *J. Am. Soc. Mass Spectrom.* **2012**, *23*, 1003–1010.
- (48) Rock, A. *Protein Express. Purif.* **2012**, *84*, 19–37.
- (49) Percy, A. J.; Rey, M.; Burns, K. M.; Schriemer, D. C. *Anal. Chim. Acta* **2012**, *721*, 7–21.
- (50) Wei, H.; Mo, J.; Tao, L.; Russell, R. J.; Tymiak, A. A.; Chen, G.; Iacob, R. E.; Engen, J. R. *Drug Discovery Today* **2013**, DOI: 10.1016/j.drudis.2013.07.019.
- (51) Rand, K. D.; Lund, F. W.; Amon, S.; Jorgensen, T. J. D. *Int. J. Mass Spectrom.* **2011**, *302*, 110–115.
- (52) Tran, D. T.; Banerjee, S.; Alayash, A. I.; Crumbliss, A. L.; Fitzgerald, J. E. *Anal. Chem.* **2012**, *84*, 1653–1660.
- (53) Guttman, M.; Scian, M.; Lee, K. K. *Anal. Chem.* **2011**, *83*, 7492–7499.
- (54) Hvilsted, A.; Nielsen, S. O. *Adv. Protein Chem.* **1966**, *21*, 287–386.
- (55) Amdursky, N.; Pecht, I.; Sheves, M.; Cahen, D. *Proc. Natl. Acad. Sci. U.S.A.* **2013**, *110*, 507–512.
- (56) Scheiner, S.; Cuma, M. *J. Am. Chem. Soc.* **1996**, *118*, 1511–1521.
- (57) Fang, J.; Rand, K. D.; Beuning, P. J.; Engen, J. R. *Int. J. Mass Spectrom.* **2011**, *302*, 19–25.
- (58) Skinner, J. J.; Lim, W. K.; Bédard, S.; Black, B. E.; Englander, S. W. *Protein Sci.* **2012**, *21*, 996–1005.
- (59) Craig, P. O.; Lätzer, J.; Weinkam, P.; Hoffman, R. M. B.; Ferreiro, D. U.; Komives, E. A.; Wolynes, P. G. *J. Am. Chem. Soc.* **2011**, *133*, 17463–17472.
- (60) Petruk, A. A.; Defelipe, L. A.; Limardo, R. G. R.; Bucci, H.; Marti, M. A.; Turjanski, A. G. *J. Chem. Theory Comput.* **2013**, *9*, 658–669.
- (61) Hsu, Y. H.; Bucher, D.; Cao, J.; Li, S.; Yang, S. W.; Kokotos, G.; Woods, V. L.; McCammon, J. A.; Dennis, E. A. *J. Am. Chem. Soc.* **2013**, *135*, 1330–1337.
- (62) Liu, T.; Pantazatos, D.; Li, S.; Hamuro, Y.; Hilser, V. J.; Woods, V. L. *J. Am. Soc. Mass Spectrom.* **2012**, *23*, 43–56.
- (63) Bai, Y.; Milne, J. S.; Mayne, L.; Englander, S. W. *Proteins: Struct., Funct., Genet.* **1993**, *17*, 75–86.
- (64) Goswami, D.; Devarakonda, S.; Chalmers, M. J.; Pascal, B. D.; Spiegelman, B. M.; Griffin, P. R. *J. Am. Soc. Mass Spectrom.* **2013**, *24*, 1584–1592.
- (65) Coales, S. J.; E, S. Y.; Lee, J. E.; Ma, A.; Morrow, J. A.; Hamuro, Y. *Rapid Commun. Mass Spectrom.* **2010**, *24*, 3585–3592.
- (66) Katta, V.; Chait, B. T. *Rapid Commun. Mass Spectrom.* **1991**, *5*, 214–217.
- (67) Zhang, Z.; Smith, D. L. *Protein Sci.* **1993**, *2*, 522–531.
- (68) Hamuro, Y. *J. Am. Soc. Mass Spectrom.* **2013**, *24*, 650–651.
- (69) Maier, C. S.; Kim, O.; Deinzer, M. L. *Anal. Biochem.* **1997**, *252*, 127–135.
- (70) Fajer, P. G.; Bou-Assaf, G. M.; Marshall, A. G. *J. Am. Soc. Mass Spectrom.* **2012**, *23*, 1202–1208.
- (71) Burns, K. M.; Rey, M.; Baker, C. A. H.; Schriemer, D. C. *Mol. Cell. Proteomics* **2013**, *12*, 539–548.
- (72) Ahn, J.; Jung, M. C.; Wyndham, K.; Yu, Y. Q.; Engen, J. R. *Anal. Chem.* **2012**, *84*, 7256–7262.
- (73) Jones, L. M.; Zhang, H.; Vidavsky, I.; Gross, M. L. *Anal. Chem.* **2010**, *82*, 1171–1174.
- (74) Venable, J. D.; Scuba, W.; Brock, A. *J. Am. Soc. Mass Spectrom.* **2013**, *24*, 642–645.
- (75) Majumdar, R.; Manikwar, P.; Hickey, J. M.; Arora, J.; Middaugh, C. R.; Volkin, D. B.; Weis, D. D. *J. Am. Soc. Mass Spectrom.* **2012**, *23*, 2140–2148.
- (76) Zhang, H. M.; McLoughlin, S. M.; Frausto, S. D.; Tang, H. L.; Emmett, M. R.; Marshall, A. G. *Anal. Chem.* **2010**, *82*, 1450–1454.
- (77) Mysling, S.; Salbo, R.; Ploug, M.; Jørgensen, T. J. D. *Anal. Chem.* **2013**, DOI: 10.1021/ac403269a.
- (78) Wales, T. E.; Fadgen, K. E.; Gerhardt, G. C.; Engen, J. R. *Anal. Chem.* **2008**, *80*, 6815–6820.
- (79) Keppel, T. R.; Jacques, M. E.; Young, R. W.; Ratzlaff, K. L.; Weis, D. D. *J. Am. Soc. Mass Spectrom.* **2011**, *22*, 1472–1476.
- (80) Kreshuk, A.; Stankiewicz, M.; Lou, X.; Kirchner, M.; Hamprecht, F. A.; Mayer, M. P. *Int. J. Mass Spectrom.* **2011**, *302*, 125–131.
- (81) Kan, Z.-Y.; Mayne, L.; Chetty, P. S.; Englander, S. W. *J. Am. Soc. Mass Spectrom.* **2011**, *22*, 1906–1915.
- (82) Zhang, Z. Q.; Zhang, A.; Xiao, G. *Anal. Chem.* **2012**, *84*, 4942–4949.
- (83) Pascal, B. D.; Willis, S.; Lauer, J. L.; Landgraf, R. R.; West, G. M.; Marciano, D.; Novick, S.; Goswami, D.; Chalmers, M. J.; Griffin, P. R. *J. Am. Soc. Mass Spectrom.* **2012**, *23*, 1512–1521.
- (84) Guttman, M.; Weis, D. D.; Engen, J. R.; Lee, K. K. *J. Am. Soc. Mass Spectrom.* **2013**, *24*, 1906–1912.
- (85) Amon, S.; Trelle, M. B.; Jensen, O. N.; Jorgensen, T. J. D. *Anal. Chem.* **2012**, *84*, 4467–4473.
- (86) Rob, T.; Gill, P. K.; Golemi-Kotra, D.; Wilson, D. *J. Lab Chip* **2013**, *13*, 2528–2532.
- (87) Mitra, G.; Muralidharan, M.; Narayanan, S.; Pinto, J.; Srinivasan, K.; Mandal, A. K. *Bioconjugate Chem.* **2012**, *23*, 2344–2353.
- (88) Sheff, J. G.; Rey, M.; Schriemer, D. C. *J. Am. Soc. Mass Spectrom.* **2013**, *24*, 1006–1015.
- (89) Venable, J. D.; Okach, L.; Agarwalla, S.; Brock, A. *Anal. Chem.* **2012**, *84*, 9601–9608.
- (90) Walters, B. T.; Ricciuti, A.; Mayne, L.; Englander, S. W. *J. Am. Soc. Mass Spectrom.* **2012**, *23*, 2132–2139.
- (91) Tan, Y. J.; Wang, W. H.; Zheng, Y.; Dong, J. L.; Stefano, G.; Brandizzi, F.; Garavito, R. M.; Reid, G. E.; Bruening, M. L. *Anal. Chem.* **2012**, *84*, 8357–8363.
- (92) Hamuro, Y.; Coales, S. J.; Molnar, K. S.; Tuske, S. J.; Morrow, J. A. *Rapid Commun. Mass Spectrom.* **2008**, *22*, 1041–1046.
- (93) Ahn, J.; Cao, M.-J.; Yu, Y. Q.; Engen, J. R. *Biochim. Biophys. Acta: Proteins Proteomics* **2013**, *1834*, 1222–1229.
- (94) Rey, M.; Yang, M. L.; Burns, K. M.; Yu, Y. P.; Lees-Miller, S. P.; Schriemer, D. C. *Mol. Cell. Proteomics* **2013**, *12*, 464–472.
- (95) Oyeyemi, O. A.; Souris, K. M.; Lee, T.; Kohen, A.; Resing, K. A.; Ahn, N. G.; Klinman, J. P. *Biochemistry* **2011**, *50*, 8251–8260.
- (96) Chalmers, M. J.; Busby, S. A.; Pascal, B. D.; West, G. M.; Griffin, P. R. *Exp. Rev. Proteomics* **2011**, *8*, 43–59.
- (97) Wei, H.; Ahn, J.; Yu, Y. Q.; Tymiak, A.; Engen, J. R.; Chen, G. J. *Am. Soc. Mass Spectrom.* **2012**, *23*, 498–504.
- (98) Choi, S. H.; Wales, T. E.; Nam, Y.; O'Donovan, D. J.; Sliz, P.; Engen, J. R.; Blacklow, S. C. *Structure* **2012**, *20*, 340–349.
- (99) Zhang, J.; Chalmers, M. J.; Stayrook, K. R.; Burris, L. L.; Wang, Y. J.; Busby, S. A.; Pascal, B. D.; Garcia-Ordonez, R. D.; Bruning, J. B.; Istrate, M. A.; Kojetin, D. J.; Dodge, J. A.; Burris, T. P.; Griffin, P. R. *Nat. Struct. Mol. Biol.* **2011**, *18*, S57.

- (100) Kim, M.; Sun, Z.-Y. J.; Rand, K. D.; Shi, X.; Song, L.; Cheng, Y.; Fahmy, A. F.; Majumdar, S.; Ofek, G.; Yang, Y.; Kwong, P. D.; Wang, J.-H.; Engen, J. R.; Wagner, G.; Reinherz, E. L. *Nat. Struct. Mol. Biol.* **2011**, *18*, 1235–1254.
- (101) Stjepanovic, G.; Kapp, K.; Bange, G.; Graf, C.; Parlitz, R.; Wild, K.; Mayer, M. P.; Sinning, I. *J. Biol. Chem.* **2011**, *286*, 23489–23497.
- (102) Powell, K. D.; Ghaemmaghami, S.; Wang, M. Z.; Ma, L.; Oas, T. G.; Fitzgerald, M. C. *J. Am. Chem. Soc.* **2002**, *124*, 10256–10257.
- (103) Zhu, M. M.; Rempel, D. L.; Du, Z. H.; Gross, M. L. *J. Am. Chem. Soc.* **2003**, *125*, 5252–5253.
- (104) Asuru, A. P.; An, M.; Busenlehner, L. S. *Biochemistry* **2012**, *51*, 7116–7127.
- (105) Sowole, M. A.; Alexopoulos, J. A.; Cheng, Y.-Q.; Ortega, J.; Konermann, L. *J. Mol. Biol.* **2013**, *425*, 4508–4519.
- (106) Abzalimov, R. R.; Bobst, C. E.; Kaltashov, I. A. *Anal. Chem.* **2013**, *85*, 9173–9180.
- (107) West, G. M.; Chien, E. Y. T.; Katritch, V.; Gatchalian, J.; Chalmers, M. J.; Stevens, R. C.; Griffin, P. R. *Structure* **2011**, *19*, 1424–1432.
- (108) Pandit, D.; Tuske, S. J.; Coales, S. J.; Yen, S.; Liu, A.; Lee, J. E.; Morrow, J. A.; Nemeth, J. F.; Hamuro, Y. *J. Mol. Recognit.* **2012**, *25*, 114–124.
- (109) Alexopoulos, J. A.; Guarnéa, A.; Ortega, J. *J. Struct. Biol.* **2012**, *179*, 202–210.
- (110) Keppel, T. R.; Howard, B. A.; Weis, D. D. *Biochemistry* **2011**, *50*, 8722–8732.
- (111) Balasubramiam, D.; Komives, E. A. *Biochim. Biophys. Acta* **2013**, *1834*, 1202–1209.
- (112) Keppel, T. R.; Weis, D. D. *Anal. Chem.* **2013**, *85*, 5161–5168.
- (113) Rob, T.; Liuni, P.; Gill, P. K.; Zhu, S. L.; Balachandran, N.; Berti, P. J.; Wilson, D. J. *Anal. Chem.* **2012**, *84*, 3771–3779.
- (114) Orban, T.; Jastrzebska, B.; Gupta, S.; Wang, B.; Miyagi, M.; Chance, M. R.; Palczewski, K. *Structure* **2012**, *20*, 826–840.
- (115) Pan, Y.; Piyadasa, H.; O’Neil, J. D.; Konermann, L. *J. Mol. Biol.* **2012**, *416*, 400–413.
- (116) Rey, M.; Forest, E.; Pelosi, L. *Biochemistry* **2012**, *51*, 9727–9735.
- (117) Mehmood, S.; Domene, C.; Forest, E.; Jault, J. M. *Proc. Natl. Acad. Sci. U.S.A.* **2012**, *109*, 10832–10836.
- (118) Pan, J.; Han, J.; Borchers, C. H.; Konermann, L. *Anal. Chem.* **2010**, *82*, 8591–8597.
- (119) Tsutsui, Y.; Dela Cruz, R. G.; Wintrode, P. L. *Proc. Natl. Acad. Sci. U.S.A.* **2012**, *109*, 4467–4472.
- (120) Zhang, Y.; Rempel, D. L.; Zhang, J.; Sharma, A. K.; Mirica, L. M.; Gross, M. L. *Proc. Natl. Acad. Sci. U.S.A.* **2013**, *110*, 14604–14609.
- (121) Hu, W. B.; Walters, B. T.; Kan, Z. Y.; Mayne, L.; Rosen, L. E.; Marqusee, S.; Englander, S. W. *Proc. Natl. Acad. Sci. U.S.A.* **2013**, *110*, 7684–7689.
- (122) Fandrich, M. *J. Mol. Biol.* **2012**, *421*, 427–440.
- (123) Sanchez, L.; Madurga, S.; Pukala, T.; Vilaseca, M.; Lopez-Iglesias, C.; Robinson, C. V.; Giralt, E.; Carulla, N. *J. Am. Chem. Soc.* **2011**, *133*, 6505–6508.
- (124) Pan, J.; Han, J.; Borchers, C. H.; Konermann, L. *Anal. Chem.* **2011**, *83*, 5386–5393.
- (125) Pan, J. X.; Han, J.; Borchers, C. H.; Konermann, L. *Biochemistry* **2012**, *51*, 3694–3703.
- (126) St. George-Hyslop, P.; Schmitt-Ulms, G. *Nature* **2010**, *467*, 36–37.
- (127) Pester, O.; Barrett, P. J.; Hornburg, D.; Hornburg, P.; Probstle, R.; Widmaier, S.; Kutzner, C.; Durrbaum, M.; Kapurniotu, A.; Sanders, C. R.; Scharnagl, C.; Langosch, D. *J. Am. Chem. Soc.* **2013**, *135*, 1317–1329.
- (128) Smirnovas, V.; Baron, G. S.; Offerdahl, D. K.; Raymond, G. J.; Caughey, B.; Surewicz, W. K. *Nat. Struct. Mol. Biol.* **2011**, *18*, 504–506.
- (129) Singh, J.; Udgaonkar, J. B. *J. Mol. Biol.* **2013**, *425*, 3510–3521.
- (130) Abzalimov, R. R.; Frimpong, A.; Kaltashov, I. A. *Int. J. Mass Spectrom.* **2012**, *312*, 135–143.
- (131) Malito, E.; Faleri, A.; Lo Surdo, P.; Veggi, D.; Maruggi, G.; Grassi, E.; Cartocci, E.; Bertoldi, I.; Genovese, A.; Santini, L.; Romagnoli, G.; Borgogni, E.; Brier, S.; Lo Passo, C.; Domina, M.; Castellino, F.; Felici, F.; van der Veen, S.; Johnson, S.; Lea, S. M.; Tang, C. M.; Pizza, M.; Savino, S.; Norais, N.; Rappuoli, R.; Bottomley, M. J.; Masignani, V. *Proc. Natl. Acad. Sci. U.S.A.* **2013**, *110*, 3304–3309.
- (132) Roder, H.; Wüthrich, K. *Proteins: Struct., Funct., Genet.* **1986**, *1*, 34–42.
- (133) Uzawa, T.; Nishimura, C.; Akiyama, S.; Ishimori, K.; Takahashi, S.; Dyson, H. J.; Wright, P. E. *Proc. Natl. Acad. Sci. U.S.A.* **2008**, *105*, 13859–13864.
- (134) Althaus, E.; Canzar, S.; Ehrler, C.; Emmett, M. R.; Karrenbauer, A.; Marshall, A. G.; Meyer-Base, A.; Tipton, J. D.; Zhang, H.-M. *BMC Bioinf.* **2010**, *11*, 424.
- (135) Kan, Z. Y.; Walters, B. T.; Mayne, L.; Englander, S. W. *Proc. Natl. Acad. Sci. U.S.A.* **2013**, *110*, 16438–16443.
- (136) Mayne, L.; Kan, Z.-Y.; Chetty, P. S.; Ricciuti, A.; Walters, B. T.; Englander, S. W. *J. Am. Soc. Mass Spectrom.* **2011**, *22*, 1898–1905.
- (137) Modzel, M.; Stefanowicz, P.; Szewczuk, Z. *Rapid Commun. Mass Spectrom.* **2012**, *26*, 2739–2744.
- (138) Rand, K. D.; Pringle, S. D.; Morris, M.; Engen, J. R.; Brown, J. M. *J. Am. Soc. Mass Spectrom.* **2011**, *22*, 1784–1793.
- (139) Yu, H. D.; Ahn, S.; Kim, B. *Bull. Korean Chem. Soc.* **2013**, *34*, 1401–1406.
- (140) Pan, J. X.; Han, J.; Borchers, C. H. *Int. J. Mass Spectrom.* **2012**, *325*, 130–138.
- (141) Pan, J.; Borchers, C. H. *Proteomics* **2013**, *13*, 974–981.
- (142) Wang, G.; Abzalimov, R. R.; Bobst, C. E.; Kaltashov, I. A. *Proc. Natl. Acad. Sci. U.S.A.* **2013**, DOI: 10.1073/pnas.1315029110.
- (143) Rand, K. D.; Bache, N.; Nedertoft, M. M.; Jørgensen, T. J. D. *Anal. Chem.* **2011**, *83*, 8859–8862.
- (144) Xian, F.; Hendrickson, C. L.; Marshall, A. G. *Anal. Chem.* **2012**, *84*, 708–719.
- (145) Landgraf, R. R.; Chalmers, M. J.; Griffin, P. R. *J. Am. Soc. Mass Spectrom.* **2012**, *23*, 301–309.
- (146) Huang, R. Y.; Garai, K.; Frieden, C.; Gross, M. L. *Biochemistry* **2011**, *50*, 9273–9282.
- (147) Mendoza, V. L.; Vachet, R. W. *Mass Spectrom. Rev.* **2009**, *28*, 785–815.
- (148) Zhou, Y.; Vachet, R. W. *J. Am. Soc. Mass Spectrom.* **2012**, *23*, 899–907.
- (149) Zheng, X.; Wintrode, P. L.; Chance, M. R. *Structure* **2008**, *16*, 38–51.
- (150) Jones, L. M.; Zhang, H.; Cui, W.; Kumar, S.; Sperry, J. B.; Carroll, J. A.; Gross, M. L. *J. Am. Soc. Mass Spectrom.* **2013**, *24*, 835–845.
- (151) Doria, F.; Nadai, M.; Folini, M.; Scalabrin, M.; Germani, L.; Sattin, G.; Mella, M.; Palumbo, M.; Zaffaroni, N.; Fabris, D.; Freccero, M.; Richter, S. N. *Chem.—Eur. J.* **2013**, *19*, 78–81.
- (152) Chen, J.; Cui, W.; Giblin, D.; Gross, M. L. *J. Am. Soc. Mass Spectrom.* **2012**, *23*, 1306–1318.
- (153) Chen, S.-H.; Russell, W. K.; Russell, D. H. *Anal. Chem.* **2013**, *85*, 229–3237.
- (154) O’Brien, J. P.; Pruet, J. M.; Brodbelt, J. S. *Anal. Chem.* **2013**, *85*, 7391–7397.
- (155) Underbakke, E. S.; Zhu, Y. M.; Kiessling, L. L. *J. Mol. Biol.* **2011**, *409*, 483–495.
- (156) Zhou, Y. P.; Vachet, R. W. *Anal. Chem.* **2013**, *85*, 9664–9670.
- (157) Xu, Y.; Falk, I. N.; Hallen, M. A.; Fitzgerald, M. C. *Anal. Chem.* **2011**, *83*, 3555–3562.
- (158) Gau, B.; Garai, K.; Frieden, C.; Gross, M. L. *Biochemistry* **2011**, *50*, 8117–8126.
- (159) Collier, T. S.; Diraviyam, K.; Monsey, J.; Shen, W.; Sept, D.; Bose, R. *J. Biol. Chem.* **2013**, *288*, 25254–25264.
- (160) Wang, L.; Chance, M. R. *Anal. Chem.* **2011**, *83*, 7234–7241.
- (161) Schorzman, A. N.; Perera, L.; Cutalo-Patterson, J. M.; Pedersen, L. C.; Pedersen, L. G.; Kunkel, T. A.; Tomer, K. B. *DNA Repair* **2011**, *10*, 454–465.
- (162) Watson, C.; Janik, L.; Zhuang, T.; Charvatova, O.; Woods, R. J.; Sharp, J. S. *Anal. Chem.* **2009**, *81*, 2496–2505.

- (163) McClintock, C. S.; Hettich, R. L. *Anal. Chem.* **2013**, *85*, 213–219.
- (164) Chen, J.; Rempel, D. L.; Gau, B.; Gross, M. L. *J. Am. Chem. Soc.* **2012**, *134*, 18724–18731.
- (165) Gau, B. C.; Chen, J. W.; Gross, M. L. *Biochim. Biophys. Acta: Proteins Proteomics* **2013**, *1834*, 1230–1238.
- (166) McClintock, C. S.; Parks, J. M.; Bern, M.; Ghatty Venkata Krishna, P. K.; Hettich, R. L. *J. Proteome Res.* **2013**, *12*, 3307–3316.
- (167) Li, X.; Li, Z.; Xie, B.; Sharp, J. S. *J. Am. Soc. Mass Spectrom.* **2013**, *24*, 1767–1776.
- (168) Jumper, C. C.; Bomgarden, R.; Rogers, J.; Etienne, C.; Schriemer, D. C. *Anal. Chem.* **2012**, *84*, 4411–4418.
- (169) Zhang, H.; Gau, B. C.; Jones, L. M.; Vidavsky, I.; Gross, M. L. *Anal. Chem.* **2011**, *83*, 311–318.
- (170) Jones, L. M.; Sperry, J. B.; Carroll, J. A.; Gross, M. L. *Anal. Chem.* **2011**, *83*, 7657–7661.
- (171) Clatterbuck Soper, S. F.; Dator, R. P.; Limbach, P. A.; Woodson, S. A. *Mol. Cell* **2013**, *52*, 506–516.
- (172) Pan, Y.; Ruan, X.; Valvano, M. A.; Konermann, L. *J. Am. Soc. Mass Spectrom.* **2012**, *23*, 889–898.
- (173) Gau, B. C.; Sharp, J. S.; Rempel, D. L.; Gross, M. L. *Anal. Chem.* **2009**, *81*, 6563–6571.
- (174) Vahidi, S.; Stocks, B. B.; Liaghati-Mobarhan, Y.; Konermann, L. *Anal. Chem.* **2013**, *85*, 8618–8625.
- (175) Jumper, C. C.; Schriemer, D. C. *Anal. Chem.* **2011**, *83*, 2913–2920.
- (176) Tucker, M. J.; Abdo, M.; Courier, J. R.; Chen, J. X.; Smith, A. B.; Hochstrasser, R. M. *J. Photochem. Photobiol., A: Chem.* **2012**, *234*, 156–163.
- (177) Lauber, M. A.; Reilly, J. P. *J. Proteome Res.* **2011**, *10*, 3604–3616.
- (178) Fischer, L.; Chen, Z. A.; Rappaport, J. *J. Proteomics* **2013**, *88*, 120–128.
- (179) Walzthoeni, T.; Leitner, A.; Stengel, F.; Aebersold, R. *Curr. Opin. Struct. Biol.* **2013**, *23*, 252–260.
- (180) Tabb, D. L. *Nat. Methods* **2012**, *9*, 879–881.
- (181) Bruce, J. E. *Proteomics* **2012**, *12*, 1565–1575.
- (182) Serpa, J. J.; Parker, C. E.; Petrotchenko, E. V.; Han, J.; Pan, J.; Borchers, C. H. *Eur. J. Mass Spectrom.* **2012**, *18*, 251–267.
- (183) Petrotchenko, E.; Borchers, C. H. *Mass Spectrom. Rev.* **2010**, *29*, 862–876.
- (184) Leitner, A.; Walzthoeni, T.; Kahraman, A.; Herzog, F.; Rinner, O.; Beck, M.; Aebersold, R. *Mol. Cell. Proteomics* **2010**, *9*, 1634–1649.
- (185) Rappaport, J. *J. Struct. Biol.* **2011**, *173*, 530–540.
- (186) Klockenbusch, C.; O'Hara, J. E.; Kast, J. *Anal. Bioanal. Chem.* **2012**, *404*, 1057–1067.
- (187) Ralton, L. D.; Murray, G. I. *J. Clin. Pathol.* **2011**, *64*, 297–302.
- (188) Koelbel, K.; Ihling, C. H.; Sinz, A. *Angew. Chem., Int. Ed.* **2012**, *51*, 12602–12605.
- (189) Schwarz, R.; Tanzler, D.; Ihling, C. H.; Muller, M. Q.; Kolbel, K.; Sinz, A. *J. Med. Chem.* **2013**, *56*, 4252–4263.
- (190) Clifford-Nunn, B.; Showalter, H. D. H.; Andrews, P. C. *J. Am. Soc. Mass Spectrom.* **2012**, *2012*, 201–212.
- (191) Walzthoeni, T.; Claassen, M.; Leitner, A.; Herzog, F.; Bohn, S.; Forster, F.; Beck, M.; Aebersold, R. *Nat. Methods* **2012**, *9*, 901.
- (192) Yang, B.; Wu, Y. J.; Zhu, M.; Fan, S. B.; Lin, J. Z.; Zhang, K.; Li, S.; Chi, H.; Li, Y. X.; Chen, H. F.; Luo, S. K.; Ding, Y. H.; Wang, L. H.; Hao, Z. Q.; Xiu, L. Y.; Chen, S.; Ye, K. Q.; He, S. M.; Dong, M. Q. *Nat. Methods* **2012**, *9*, 904.
- (193) Kahraman, A.; Herzog, F.; Leitner, A.; Rosenberger, G.; Aebersold, R.; Malmstrom, L. *PLoS One* **2013**, DOI: 10.1371/journal.pone.0073411.
- (194) Herzog, F.; Kahraman, A.; Boehringer, D.; Mak, R.; Bracher, A.; Walzthoeni, T.; Leitner, A.; Beck, M.; Hartl, F. U.; Ban, N.; Malmstrom, L.; Aebersold, R. *Science* **2012**, *337*, 1348–1352.
- (195) Chavez, J. D.; Weisbrod, C. R.; Zheng, C. X.; Eng, J. K.; Bruce, J. E. *Mol. Cell. Proteomics* **2013**, *12*, 1451–1467.
- (196) Weisbrod, C. R.; Chavez, J. D.; Eng, J. K.; Yang, L.; Zheng, C. X.; Bruce, J. E. *J. Proteome Res.* **2013**, *12*, 1569–1579.
- (197) Chowdhury, S. K.; Katta, V.; Chait, B. T. *J. Am. Chem. Soc.* **1990**, *112*, 9012–9013.
- (198) Testa, L.; Brocca, S.; Grandori, R. *Anal. Chem.* **2011**, *83*, 6459–6463.
- (199) Douglass, K. A.; Venter, A. R. *Anal. Chem.* **2013**, *85*, 8212–8218.
- (200) Shepherd, D. A.; Holmes, K.; Rowlands, D. J.; Stonehouse, N. J.; Ashcroft, A. E. *Biophys. J.* **2013**, *105*, 1258–1267.
- (201) Hamdy, O. M.; Julian, R. R. *J. Am. Soc. Mass Spectrom.* **2012**, *23*, 1–6.
- (202) Konermann, L.; Ahadi, E.; Rodriguez, A. D.; Vahidi, S. *Anal. Chem.* **2013**, *85*, 2–9.
- (203) Kebarle, P.; Verkerk, U. H. *Mass Spectrom. Rev.* **2009**, *28*, 898–917.
- (204) Dole, M.; Mack, L. L.; Hines, R. L.; Mobley, R. C.; Ferguson, L. D.; Alice, M. B. *J. Chem. Phys.* **1968**, *49*, 2240–2249.
- (205) de la Mora, F. J. *Anal. Chim. Acta* **2000**, *406*, 93–104.
- (206) Hogan, C. J.; Carroll, J. A.; Rohrs, H. W.; Biswas, P.; Gross, M. L. *Anal. Chem.* **2009**, *81*, 369–377.
- (207) Allen, S. J.; Schwartz, A. M.; Bush, M. F. *Anal. Chem.* **2013**, DOI: 10.1021/ac403139d.
- (208) Marchese, R.; Grandori, R.; Carloni, R.; Raugei, S. *J. Am. Soc. Mass Spectrom.* **2012**, *23*, 1903–1910.
- (209) Freeke, J.; Bush, M. F.; Robinson, C. V.; Ruotolo, B. T. *Chem. Phys. Lett.* **2012**, *524*, 1–9.
- (210) Sciuto, S. V.; Liu, J.; Konermann, L. *J. Am. Soc. Mass Spectrom.* **2011**, *22*, 1679–1689.
- (211) Fegan, S. K.; Thachuk, M. *J. Chem. Theory Comput.* **2013**, *9*, 2531–2539.
- (212) Zhou, M.; Dagan, S.; Wysocki, V. H. *Analyst* **2013**, *138*, 1353–1362.
- (213) Chung, J. K.; Consta, S. *J. Phys. Chem. B* **2012**, *116*, 5777–5785.
- (214) Abzalimov, R. R.; Frimpong, A. K.; Kaltashov, I. A. *Int. J. Mass Spectrom.* **2006**, *253*, 207–216.
- (215) Zhou, M.; Dagan, S.; Wysocki, V. H. *Angew. Chem., Int. Ed.* **2012**, *51*, 4336–4339.
- (216) Lin, H.; Kitova, E. N.; Johnson, M. A.; Eugenio, L.; Ng, K. K. S.; Klassen, J. S. *J. Am. Soc. Mass Spectrom.* **2012**, *23*, 2122–2131.
- (217) Girod, M.; Dagany, X.; Boutou, V.; Broyer, M.; Antoine, R.; Dugourd, P.; Mordehai, A.; Love, C.; Werlich, M.; Fjeldsted, J.; Stafford, G. *Phys. Chem. Chem. Phys.* **2012**, *14*, 9389–9396.
- (218) Lomeli, S. H.; Peng, I. X.; Yin, S.; Ogorzalek Loo, R. R.; Loo, J. A. *J. Am. Soc. Mass Spectrom.* **2010**, *21*, 127–131.
- (219) Sterling, H. J.; Prell, J. S.; Cassou, C. A.; Williams, E. R. *J. Am. Soc. Mass Spectrom.* **2011**, *22*, 1178–1186.
- (220) Hedges, J. B.; Vahidi, S.; Yue, X.; Konermann, L. *Anal. Chem.* **2013**, *85*, 6469–6476.
- (221) Cassou, C. A.; Sterling, H. J.; Susa, A. C.; Williams, E. R. *Anal. Chem.* **2013**, *85*, 138–146.
- (222) Iavarone, A. T.; Williams, E. R. *J. Am. Chem. Soc.* **2003**, *125*, 2319–2327.
- (223) Samalikova, M.; Grandori, R. *J. Am. Chem. Soc.* **2003**, *125*, 13352–13353.
- (224) Girod, M.; Antoine, R.; Dugourd, P.; Love, C.; Mordehai, A.; Stafford, G. *J. Am. Soc. Mass Spectrom.* **2012**, *23*, 1221–1231.
- (225) Kharlamova, A.; McLuckey, S. A. *Anal. Chem.* **2011**, *83*, 431–437.
- (226) Sokratous, K.; Roach, L. V.; Channing, D.; Strachan, J.; Long, J.; Searle, M. S.; Layfield, R.; Oldham, N. J. *J. Am. Chem. Soc.* **2012**, *134*, 6416–6424.
- (227) Ferguson, C. N.; Benchaar, S. A.; Miao, Z. X.; Loo, J. A.; Chen, H. *Anal. Chem.* **2011**, *83*, 6468–6473.
- (228) Jackson, S. N.; Woods, A. S. *J. Am. Soc. Mass Spectrom.* **2013**, *24*, 1950–1956.
- (229) Pacholarz, K. J.; Garlish, R. A.; Taylor, R. J.; Barran, P. E. *Chem. Soc. Rev.* **2012**, *41*, 4335–4355.
- (230) Woods, L. A.; Radford, S. E.; Ashcroft, A. E. *Biochim. Biophys. Acta* **2013**, *1834*, 1257–1268.

- (231) Williams, D. M.; Pukala, T. L. *Mass Spectrom. Rev.* **2013**, *32*, 169–187.
- (232) Zhong, Y.; Hyung, S.-J.; Ruotolo, B. T. *Exp. Rev. Proteomics* **2012**, *9*, 47–58.
- (233) Sharon, M. *Science* **2013**, *340*, 1059–1060.
- (234) Marcoux, J.; Robinson, C. V. *Structure* **2013**, *21*, 1541–1550.
- (235) Hilton, G. R.; Benesch, J. L. P. *J. R. Soc. Interface* **2012**, *9*, 801–816.
- (236) Bakker, H. J. *Nature* **2012**, *491*, 533–535.
- (237) Lin, M. M.; Zewail, A. H. *Proc. Natl. Acad. Sci. U.S.A.* **2012**, *109*, 9851–9856.
- (238) Warnke, S.; von Helden, G.; Pagel, K. *J. Am. Chem. Soc.* **2013**, *135*, 1177–1180.
- (239) Frankevich, V.; Barylyuk, K.; Chingin, K.; Nieckarz, R.; Zenobi, R. *ChemPhysChem* **2013**, *14*, 929–935.
- (240) Ly, T.; Julian, R. R. *J. Am. Chem. Soc.* **2010**, *132*, 8602–8609.
- (241) Hall, Z.; Politis, A.; Bush, M. F.; Smith, L. J.; Robinson, C. V. *J. Am. Chem. Soc.* **2012**, *134*, 3429–3438.
- (242) Balthasar, F.; Plavec, J.; Gabelica, V. *J. Am. Soc. Mass Spectrom.* **2013**, *24*, 1–8.
- (243) Ruotolo, B. T.; Robinson, C. V. *Curr. Opin. Chem. Biol.* **2006**, *10*, 402–408.
- (244) Vahidi, S.; Stocks, B. B.; Konermann, L. *Anal. Chem.* **2013**, *85*, 10471–10478.
- (245) Arcella, A.; Portella, G.; Ruiz, M. L.; Eritja, R.; Vilaseca, M.; Gabelica, V.; Orozco, M. *J. Am. Chem. Soc.* **2012**, *134*, 6596–6606.
- (246) Bush, M. F.; Hall, Z.; Giles, K.; Hoyes, J.; Robinson, C. V.; Ruotolo, B. T. *Anal. Chem.* **2010**, *82*, 9667–9565.
- (247) Bohrer, B. C.; Atlasevich, N.; Clemmer, D. E. *J. Phys. Chem. B* **2011**, *115*, 4509–4515.
- (248) Kang, Y.; Terrier, P.; Ding, C.; Douglas, D. J. *J. Am. Soc. Mass Spectrom.* **2012**, *23*, 57–67.
- (249) Rand, K. D.; Pringle, S. D.; Morris, M.; Brown, J. M. *Anal. Chem.* **2012**, *84*, 1931–1940.
- (250) Pan, J.; Heath, B. L.; Jockusch, R. A.; Konermann, L. *Anal. Chem.* **2012**, *84*, 373–378.
- (251) McGee, W. M.; Mentinova, M.; McLuckey, S. A. *J. Am. Chem. Soc.* **2012**, *134*, 11412–11414.
- (252) Prentice, B. M.; Gilbert, J. D.; Stutzman, J. R.; Forrest, W. P.; McLuckey, S. A. *J. Am. Soc. Mass Spectrom.* **2013**, *24*, 30–37.
- (253) Mentinova, M.; McLuckey, S. A. *J. Am. Soc. Mass Spectrom.* **2011**, *22*, 912–921.
- (254) Talbot, F. O.; Rullo, A.; Yao, H.; Jockusch, R. A. *J. Am. Chem. Soc.* **2010**, *132*, 16156–16164.
- (255) Le, T. N.; Pouilly, J. C.; Lecomte, F.; Nieuwjaer, N.; Manil, B.; Desfrançois, C.; Chirot, F.; Lemoine, J.; Dugourd, P.; van der Rest, G.; Grégoire, G. *J. Am. Soc. Mass Spectrom.* **2013**, *24*, 1937–1949.
- (256) Stedwell, C. N.; Galindo, J. F.; Roitberg, A. E.; Polfer, N. C. *Annu. Rev. Anal. Chem.* **2013**, *6*, 267–285.
- (257) Yao, H.; Jockusch, R. A. *J. Phys. Chem. A* **2013**, *117*, 1351–1359.
- (258) Breuker, K.; Brüschweiler, S.; Tollinger, M. *Angew. Chem., Int. Ed.* **2011**, *50*, 873–877.
- (259) Zhang, H.; Wen, J.; Blankenship, R. E.; Gross, M. L. *Anal. Chem.* **2011**, *83*, 5598–5606.
- (260) Bohrer, B. C.; Merenbloom, S. I.; Koeniger, S. L.; Hilderbrand, A. E.; Clemmer, D. E. *Annu. Rev. Anal. Chem.* **2008**, *1*, 293–327.
- (261) Giles, K.; Williams, J. P.; Campuzano, I. *Rapid Commun. Mass Spectrom.* **2011**, *25*, 1559–1566.
- (262) Silveira, J. A.; Servage, K. A.; Gamage, C. M.; Russell, D. H. *J. Phys. Chem. A* **2013**, *117*, 953–961.
- (263) Glaskin, R. S.; Ewing, M. A.; Clemmer, D. E. *Anal. Chem.* **2013**, *85*, 7003–7008.
- (264) Shvartsburg, A. A.; Smith, R. D. *Anal. Chem.* **2013**, *85*, 10–13.
- (265) Bush, M. F.; Campuzano, I. D. G.; Robinson, C. V. *Anal. Chem.* **2012**, *84*, 7124–7130.
- (266) Ruotolo, B. T.; Benesch, J. L. P.; Sandercock, A. M.; Hyung, S.-J.; Robinson, C. V. *Nat. Protoc.* **2008**, *3*, 1139–1152.
- (267) Mesleh, M. F.; Hunter, J. M.; Shvartsburg, A. A.; Schatz, G. C.; Jarrold, M. F. *J. Phys. Chem.* **1996**, *100*, 16082–16086.
- (268) Jurneczko, E.; Barran, P. E. *Analyst* **2011**, *136*, 20–28.
- (269) Williams, J. P.; Lough, J. A.; Campuzano, I.; Richardson, K.; Sadler, P. J. *Rapid Commun. Mass Spectrom.* **2009**, *23*, 3563–3569.
- (270) Pierson, N. A.; Chen, L.; Russell, D. H.; Clemmer, D. E. *J. Am. Chem. Soc.* **2013**, *135*, 3186–3192.
- (271) Rabuck, J. N.; Hyung, S.-J.; Ko, K. S.; Fox, C. C.; Soellner, M. B.; Ruotolo, B. T. *Anal. Chem.* **2013**, *85*, 6995–7002.
- (272) Hogan, C. J.; Ruotolo, B. T.; Robinson, C. V.; de la Mora, J. F. *J. Phys. Chem. B* **2011**, *115*, 3614–3621.
- (273) Wyttenbach, T.; Bleiholder, C.; Bowers, M. T. *Anal. Chem.* **2013**, *85*, 2191–2199.
- (274) Chen, Y.-L.; Collings, B. A.; Douglas, D. J. *J. Am. Soc. Mass Spectrom.* **1997**, *8*, 681–687.
- (275) Fitzgerald, M. C.; Chernushevich, I.; Standing, K. G.; Whitman, C. P.; Kent, S. B. H. *Proc. Natl. Acad. Sci. U.S.A.* **1996**, *93*, 6851–6856.
- (276) Kozlovski, V. I.; Donald, L. J.; Collado, V. M.; Spicer, V.; Loboda, A. V.; Chernushevich, I. V.; Ens, W.; Standing, K. G. *Int. J. Mass Spectrom.* **2011**, *308*, 118–125.
- (277) Snijder, J.; Rose, R. J.; Veesler, D.; Johnson, J. E.; Heck, A. J. R. *Angew. Chem., Int. Ed.* **2013**, *52*, 4020–4023.
- (278) Utrecht, C.; Heck, A. J. R. *Angew. Chem., Int. Ed.* **2011**, *50*, 8248–8262.
- (279) Utrecht, C.; Barbu, I. M.; Shoemaker, G. K.; van Duijn, E.; Heck, A. J. R. *Nat. Chem.* **2011**, *3*, 126–132.
- (280) Santambrogio, C.; Sperandeo, P.; Villa, R.; Sobott, F.; Polissi, A.; Grandori, R. *J. Am. Soc. Mass Spectrom.* **2013**, *24*, 1593–1602.
- (281) Debaene, F.; Wagner-Rousset, E.; Colas, O.; Ayoub, D.; Corvaia, N.; Van Dorsselaer, A.; Beck, A. H.; Cianfarani, S. *Anal. Chem.* **2013**, *85*, 9785–9792.
- (282) Bleiholder, C.; Dupuis, N. F.; Wyttenbach, T.; Bowers, M. T. *Nat. Chem.* **2011**, *3*, 172–177.
- (283) Woods, L. A.; Platt, G. W.; Hellewell, A. L.; Hewitt, E. W.; Homans, S. W.; Ashcroft, A. E.; Radford, S. E. *Nat. Chem. Biol.* **2011**, *7*, 730–739.
- (284) Housden, N. G.; Hopper, J. T. S.; Lukyanova, N.; Rodriguez-Larrea, D.; Wojdyla, J. A.; Klein, A.; Kaminska, R.; Bayley, H.; Saibil, H. R.; Robinson, C. V.; Kleanthous, C. *Science* **2013**, *340*, 1570–1574.
- (285) Laganowsky, A.; Reading, E.; Hopper, J. T. S.; Robinson, C. V. *Nat. Protoc.* **2013**, *8*, 639–651.
- (286) Zhou, M.; Morgner, N.; Barrera, N. P.; Politis, A.; Isaacson, S. C.; Mata-Vinkovic, D.; Murata, T.; Bernal, R. A.; Stock, D.; Robinson, C. V. *Science* **2011**, *334*, 380–385.
- (287) Leney, A. C.; McMorrin, L. M.; Radford, S. E.; Ashcroft, A. E. *Anal. Chem.* **2012**, *84*, 9841–9847.
- (288) Marty, M. T.; Zhang, H.; Cui, W. D.; Blankenship, R. E.; Gross, M. L.; Sligar, S. G. *Anal. Chem.* **2012**, *84*, 8957–8960.
- (289) Hopper, J. T. S.; Yu, Y. T.-C.; Li, D.; Raymond, A.; Bostock, M.; Liko, I.; Mikhailov, V.; Laganowsky, A.; Benesch, J. L. P.; Caffrey, M.; Nietlispach, D.; Robinson, C. V. *Nat. Methods* **2013**, *10*, 1206–1208.
- (290) Morgner, N.; Robinson, C. V. *Curr. Opin. Struct. Biol.* **2012**, *22*, 44–51.
- (291) Bornschein, R. E.; Hyung, S.-J.; Ruotolo, B. T. *J. Am. Soc. Mass Spectrom.* **2011**, *22*, 1690–1698.
- (292) Borysik, A. J.; Hewitt, D. J.; Robinson, C. V. *J. Am. Chem. Soc.* **2013**, *135*, 6078–6083.
- (293) Cubrilovic, D.; Biela, A.; Sielaff, F.; Steinmetzer, T.; Klebe, G.; Zenobi, R. *J. Am. Soc. Mass Spectrom.* **2012**, *23*, 1768–1777.
- (294) Han, L.; Hyung, S.-J.; Mayers, J. J. S.; Ruotolo, B. T. *J. Am. Chem. Soc.* **2011**, *133*, 11358–11367.
- (295) Han, L.; Hyung, S.-J.; Ruotolo, B. T. *Angew. Chem., Int. Ed.* **2012**, *51*, 5692–5695.
- (296) Politis, A.; Park, A. Y.; Hyung, S.-J.; Barsky, D.; Ruotolo, B. T.; Robinson, C. V. *PLoS One* **2010**, *5*, e12080.
- (297) Zhou, M.; Jones, C. M.; Wysocki, V. H. *Anal. Chem.* **2013**, *85*, 8262–8267.

- (298) Hall, Z.; Politis, A.; Robinson, C. V. *Structure* **2012**, *20*, 1596–1609.
- (299) Dyachenko, A.; Gruber, R.; Shimon, L.; Horovitz, A.; Sharon, M. *Proc. Natl. Acad. Sci. U.S.A.* **2013**, *110*, 7235–7239.
- (300) Tiedemann, M. T.; Heinrichs, D. E.; Stillman, M. J. *J. Am. Chem. Soc.* **2012**, *134*, 16578–16585.
- (301) Seo, Y.; Andaya, A.; Bleiholder, C.; Leary, J. A. *J. Am. Chem. Soc.* **2013**, *135*, 4325–4332.
- (302) Kitova, E. N.; El-Hawiet, A.; Schnier, P. D.; Klassen, J. S. *J. Am. Soc. Mass Spectrom.* **2012**, *23*, 431–441.
- (303) Jaquillard, L.; Saab, F.; Schoentgen, F.; Cadene, M. *J. Am. Soc. Mass Spectrom.* **2012**, *23*, 908–922.
- (304) Bich, C.; Baer, S.; Jecklin, M. C.; Zenobi, R. *J. Am. Soc. Mass Spectrom.* **2010**, *21*, 286–289.
- (305) Barylyuk, K.; Balabin, R. M.; Grunstein, D.; Kikkeri, R.; Frankevich, V.; Seeberger, P. H.; Zenobi, R. *J. Am. Soc. Mass Spectrom.* **2011**, *22*, 1167–1177.
- (306) Liu, L.; Kitova, E. N.; Klassen, J. S. *J. Am. Soc. Mass Spectrom.* **2011**, *22*, 310–318.
- (307) Cubrilovic, D.; Zenobi, R. *Anal. Chem.* **2013**, *85*, 2724–2730.
- (308) El-Hawiet, A.; Kitova, E. N.; Arutyunov, D.; Simpson, D. J.; Szymanski, C. M.; Klassen, J. S. *Anal. Chem.* **2012**, *84*, 3867–3870.
- (309) Zhang, Y. X.; Liu, L.; Daneshfar, R.; Kitova, E. N.; Li, C. S.; Jia, F.; Cairo, C. W.; Klassen, J. S. *Anal. Chem.* **2012**, *84*, 7618–7621.
- (310) Lin, H.; Kitova, E. N.; Klassen, J. S. *Anal. Chem.* **2013**, *85*, 8919–8922.
- (311) Su, H. F.; Xue, L.; Li, Y. H.; Lin, S. C.; Wen, Y. M.; Huang, R. B.; Xie, S. Y.; Zheng, L. S. *J. Am. Chem. Soc.* **2013**, *135*, 6122–6129.
- (312) Clarke, D. J.; Murray, E.; Hupp, T.; Mackay, C. L.; Langridge-Smith, P. R. R. *J. Am. Soc. Mass Spectrom.* **2011**, *22*, 1432–1440.
- (313) Yin, S.; Loo, J. A. *Int. J. Mass Spectrom.* **2011**, *300*, 118–122.
- (314) Sterling, H. J.; Kintzer, A. F.; Feld, G. K.; Cassou, C. A.; Krantz, B. A.; Williams, E. R. *J. Am. Soc. Mass Spectrom.* **2012**, *23*, 191–200.
- (315) Enyenih, A. A.; Yang, H.; Ytterberg, A. J.; Lyutvinskiy, Y.; Zubarev, A. R. *J. Am. Soc. Mass Spectrom.* **2011**, *22*, 1763–1770.
- (316) Heath, B. L.; Jockusch, R. A. *J. Am. Soc. Mass Spectrom.* **2012**, *23*, 1911–1920.
- (317) Rozbesky, D.; Man, P.; Kavan, D.; Chmelik, J.; Cerny, J.; Bezouska, K.; Novak, P. *Anal. Chem.* **2012**, *84*, 867–870.
- (318) Serpa, J. J.; Patterson, A. P.; Pan, J. X.; Han, J.; Wishart, D. S.; Petrotchenko, E. V.; Borchers, C. H. *J. Proteomics* **2013**, *81*, 31–42.
- (319) Bogan, M. J. *Anal. Chem.* **2013**, *85*, 3464–3471.
- (320) Wang, B.; Trimpin, S. *Anal. Chem.* **2013**, DOI: 10.1021/ac400867b.